SIMULATION AND ANALYSIS OF WELLBORE STABILITY IN PERMAFROST FORMATION WITH FLAC

By

Kai Wang

Dr. Shirish Patil, Advisory Committee Chair
Petroleum Engineering Department

Dr. Gang Chen, Advisory Committee Co-Chair
Mining and Geological Engineering Department

Dr. Abhijit Dandekar, Advisory Committee Member
Petroleum Engineering Department

Dr. Santanu Khataniar, Advisory Committee Member
Petroleum Engineering Department

Summer 2015

Simulation and Analysis of Wellbore Stability in Permafrost Formation with FLAC

A PROJECT REPORT

Submitted to the Department of Petroleum Engineering

University of Alaska Fairbanks

in Partial Fulfillment of the Requirements

for the Degree of

MASTER OF SCIENCE

By

Kai Wang

Fairbanks, Alaska

July 2015

Abstract

Permafrost underlies approximately 80% of Alaska. Permafrost's high sensitivity to temperature variations plays a significant role in the stability of wellbores drilled through permafrost formations. Wellbore instability may cause stuck pipes, lost circulation, and/or collapse of the wellbore, resulting in extra cost and time loss. In order to minimize the influence of the heat produced during drilling, a vertical well is the only choice to penetrate permafrost formation.

Fast Lagrangian Analysis of Continua (FLAC) was used in this simulation to test the minimum wellbore pressure to maintain stability in a permafrost formation. Three layers were set in the simulation model: clay, silt, and sand. With the drilling fluid temperature set at 343K and a 267K initial formation temperature, four different thermal times, i.e. 1 week, 1 month, 1 year, and 5 years, were tested to determine the minimum stable pressure. Pore pressure of the formation has the strongest effect on this pressure. And in a short operation period, drilling fluid temperature will not influence the minimum mud pressure value significantly.

A regression analysis was conducted on the simulation results, and the minimum wellbore stable pressure was found to be a function of pore pressure, cohesion, frictional angle, temperature difference, conductivity difference, thermal time, and wellbore radius. With the help of this function, engineers could calculate stable pressure for wells in arctic area before drilling based on drilling fluid temperature.

Table of Contents

page

Signature Page....i

Title Page....iii

Abstract....v

Table of Contents....vi

List of Figures....viii

List of Tables....x

Acknowledgement....xi

Chapter 1: Introduction to Permafrost and Wellbore Instability....1

1.1 Permafrost Definition and Background....1
1.2 Permafrost General Distribution and Classification....2
1.3 Active Layer....4
1.4 Factors Influencing Permafrost....4
1.5 Thermal History of Permafrost in Alaska....6
1.6 Wellbore Instability....8
1.6.1 Causes of Wellbore Instability....8
1.6.2 Bottom-Hole Pressure....9
1.6.3 Wellbore Instability Indicators....10
1.7 Problems for Arctic Wells....10
1.7.1 Thaw Subsidence....12
1.7.2 Internal and External Freezeback....13
1.7.3 Other Problems....14

Chapter 2: Stress and Strain around the Wellbore and in Frozen Soil....15

2.1 Stress and Strain....15
2.2 Principal Stress and In-situ Stress....17
2.3 Stresses around the Wellbore....18
2.4 Creep of Frozen Soil....20

Chapter 3: Properties of Permafrost....22

3.1 Water Content....22
3.2 Cohesion....22
3.3 Young's Modulus....23
3.4 Volumetric Heat Capacity and Latent Heat of Fusion....24
3.5 Thermal Conductivity....25

Chapter 4: Simulation of a Vertical Well in Permafrost with FLAC....29

4.1 Data Used in Simulation....29
4.2 Simulation Procedures and Model Build....33

Chapter 5: Simulation Results and Analysis....41

5.1 Simulation Results....41
5.2 Regression Analysis of Results....51
5.3 Stable Pressure after Casing Added....52
Chapter 6: Conclusions and Recommendations....54
6.1 Conclusions....54
6.2 Recommendations....55
Appendix....56
Appendix I: FLAC Code Explanation....56
Appendix II: FLAC Code Examples for Simulation....56
References....65

LIST OF FIGURES

page

Figure 1 Permafrost in the Northern Hemisphere....2
Figure 2 Occurrence of Terrestrial Permafrost....3
Figure 3 Time series of temperatures....7
Figure 4 Types of Wellbore Instability....8
Figure 5 Effect of Mud Weight on the Stress in Wellbore Wall....9
Figure 6 Radii of Thaw around a Conventional Production Well....11
Figure 7 Schematic of Thaw-Consolidation Process....12
Figure 8 Stress Components of the Normal and Shear Stress....15
Figure 9 Center to Center distances....16
Figure 10 Displacement Produced by Normal and Shear Strain....17
Figure 11 Schematic In-situ Stress and Associated Fault Types....18
Figure 12 Schematic of Stresses around a Vertical Well....19
Figure 13 Stress and Strain in Constant Stress Creep Test....21
Figure 14 Schematic Plots of Data from Compression Creep Tests....21
Figure 15 Temperature Dependence of UCS for Various Frozen Materials....23
Figure 16 Schematic of Heat Capacity and Latent Heat....25
Figure 17 Average Thermal Conductivity for Sands and Gravels....27
Figure 18 Average Thermal Conductivity for Silt and Clay....28
Figure 19 Cohesions of Different Materials at Negative Temperature....30
Figure 20 Temperature Distribution of Sand....36
Figure 21 Temperature Distribution of Silt....37
Figure 22 Temperature Distribution of Clay....38
Figure 23 State of Wellbore in Sand Applying 2.4 MPa....39
Figure 24 State of Wellbore in Sand Applying 2.3 MPa....40
Figure 25 Initial Elastic Graph of Silt at 280m Depth....41
Figure 26 Elastic Graph Shows Yield far from the Wellbore....42
Figure 27 Clay Shows Little Yield Point Around the Wellbore....43
Figure 28 Thaw Radii Difference between Simulation and Reference....50

Figure 29 Clay Shows No Yield Point after Casing Added.....53

LIST OF TABLES

page

Table 1: Causes of Wellbore Instability....9
Table 2: Indicators of Wellbore Instability....10
Table 3: Thermal Properties of Selected materials....25
Table 4: UCS and Cohesion of Different Materials at Specific Friction Angle....30
Table 5: Young's modulus of Different Materials....31
Table 6: Horizontal Stresses and Pore Pressure for the Simulation....32
Table 7: Frozen and Unfrozen Thermal Conductivity of Different Materials....33
Table 8: Input Parameters for Initial Mechanical Analysis....33
Table 9: Minimum Stable Pressure at Thermal Time 1 week....44
Table 10: Minimum Stable Pressure at Thermal Time 1 month....45
Table 11: Minimum Stable Pressure at Thermal Time 1 year....47
Table 12: Minimum Stable Pressure at Thermal Time 5 years....48
Table 13: Property Change Influence Tested Pressure....51
Table 14: Regression Analysis Result....51

Acknowledgement

First and foremost, I would like to show my deepest gratitude to all of my committee member, Dr. Shirish Patil, Dr. Gang Chen, Dr. Abhijit Dandekar, and Dr. Santanu Khataniar. They provided me with valuable guidance in every stage of this project. Without their enlightening instruction, impressive kindness and patience, I could not have completed my thesis.

I shall extend my thanks to Dr. Yanhui Han. He checked my FLAC code and helps me a lot to correct the simulation model. Also, I appreciate with the help from Dr. Yuri Shur, Dr. Matt Bray, and Chuang Lin. They provide me guidance to get permafrost properties values.

Last but not least, I'd like to thanks Sue Beck with the report corrections and Yanan Hu who help me to edit figures in this report.

Chapter 1: Introduction to Permafrost and Wellbore Instability

1.1 Permafrost Definition and Background

The word *permafrost* was first introduced by S.W. Muller in 1945 as a translation of the Russian for "permanently frozen ground (soil)". The definition of permafrost is ground whose temperature remains below 0°C for at least two consecutive years (Ferrians 1994). This definition is used in the English-language literature. The Russian definition of permafrost is different. The main difference between the Russian and English definitions of permafrost is the occurrence of ice in the ground.

Permafrost by the English definition is not perennially frozen ground. According to Shur (2014), permafrost is not necessarily frozen, because the freezing point of the included water may be depressed several degrees below 0°C; moisture in the form of ice may or may not be present. In other words, whereas all perennially frozen ground is permafrost, not all permafrost is perennially frozen.

Based on that definition, permafrost forms when the mean annual air temperature is low enough to maintain mean annual near-surface temperature at or below 0°C. The first permafrost must have existed prior to or have formed with the first glaciation, approximately 2.3 billion years ago. As permafrost increases in cold climates and decreases during warm intervals, the Arctic permafrost may have disappeared 50 million years ago. The permafrost of Alaska that exists today formed around 2.5 million years ago, during the climatic cooling period (Jorgenson and Osterkamp 2009).

There are two main categories of permafrost formation according to Yuri Shur's course ware (2014). One is epigenetic permafrost, which forms by the freezing of soil or rock downward from the bottom of the active layer after deposition of the soil sequence. The time lag between soil accumulation and its perennial freezing can be thousands or millions of years. Syngenetic permafrost is the other, the formation

which takes place simultaneously with the deposition of the soil material and follows this deposition in the same direction.

1.2 Permafrost General Distribution and Classification

From Ferrian's paper (1994), Permafrost underlies approximately one quarter of the world's land surface. More than 60% of Russia, more than 50% of Canada, 20% of the People's Republic of China and more than 80% of the land area in Alaska is underlain by permafrost.

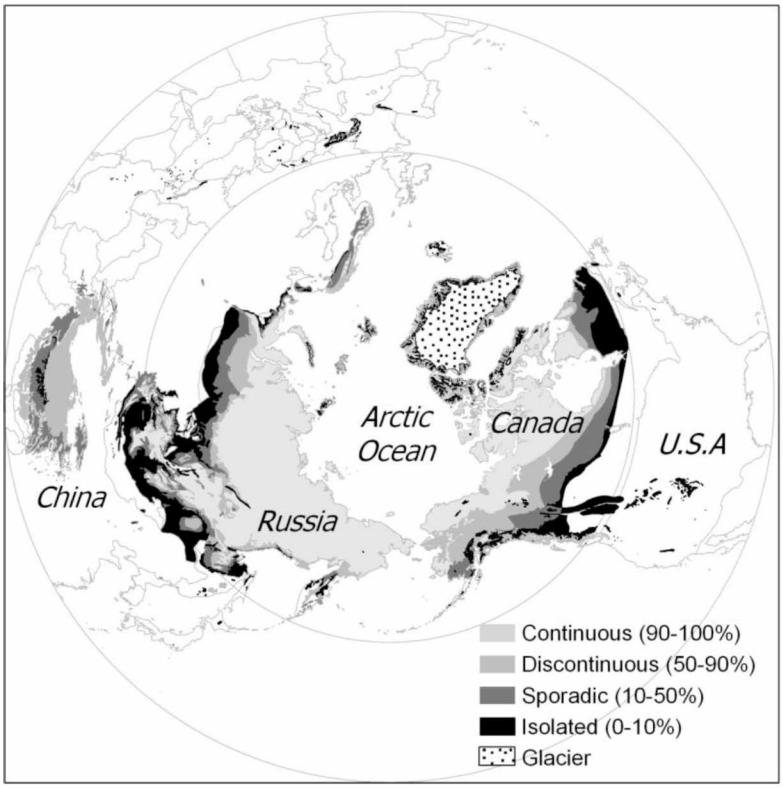

Figure 1. Permafrost in the Northern Hemisphere (Shur 2014)

According to Ferrians, the Soviets during the 1930s and 1940s were the first to use a system to divide the permafrost region into three zones: (1) the continuous permafrost zone, which is underlain by permafrost almost everywhere except under large water bodies that are deep enough not to freeze to the bottom during winter; (2) the discontinuous permafrost zone, where some areas have permafrost and other areas are free of it; and (3) the sporadic permafrost zone, which is mostly permafrost free, but numerous areas do have permafrost. The discontinuous and sporadic zones can be

defined with the help of permafrost temperatures. For discontinuous permafrost, the temperature is from -5°C to -1°C and for sporadic permafrost the temperature is higher than -1°C. The occurrence of terrestrial permafrost is shown in Figure 2.

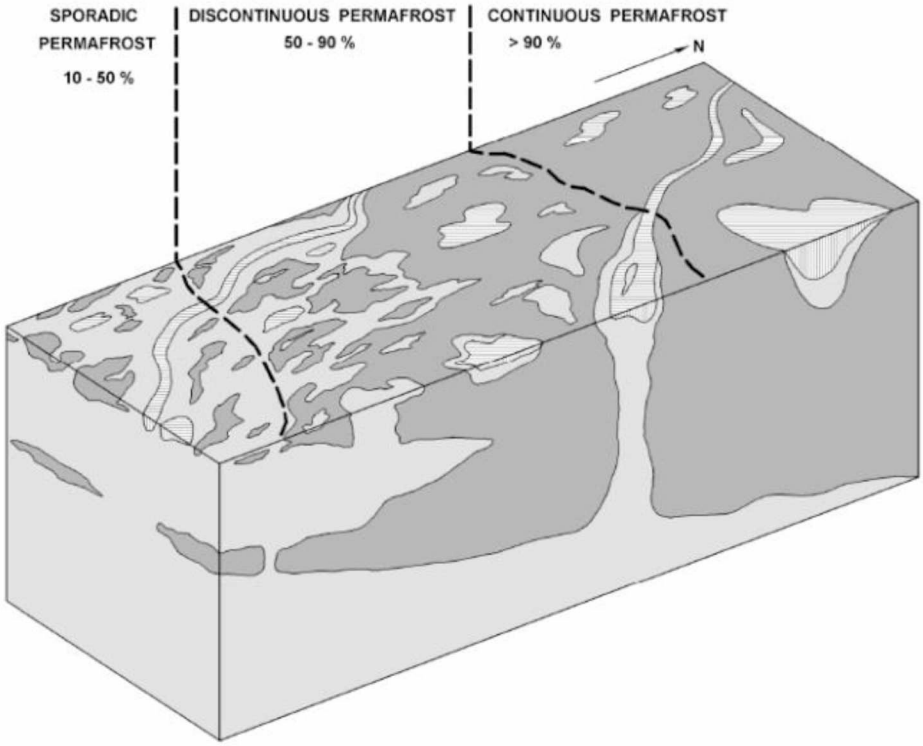

Figure 2. Occurrence of Terrestrial Permafrost (Shur 2014)

From my "Introduction of Permafrost Engineering" courseware, another kind of permafrost that is important for petroleum engineers is called subsea (offshore) permafrost. The existence of this kind of permafrost is possibly because mean annual sea water temperature in the Arctic is generally below 0°C. The three ways that subsea permafrost forms are: (1) onshore during regression by interaction with the atmosphere; (2) offshore under bottom-fast ice; (3) from subsurface remnants of eroded island.

The exact extent of subsea permafrost is not known. Preliminary estimation shows that it could be greater than 10,000,000 square kilometers. The area of ice-bearing permafrost is much smaller. The thickness of subsea permafrost at some places estimated as several hundreds of meters.

1.3 Active Layer

Active layer is a very important component in permafrost formations. The active layer can be understood as the insulative layer protecting permafrost. The mean annual temperature at the bottom of the active layer changes from year to year. At the southern margin of the permafrost region, these changes can lead to formation of a temporary layer of permafrost, or to formation of a residual thawed layer between the bottom of the active layer and the permafrost table. The definition of active layer from Yuri Shur's course ware (2014) is that layer of the ground that is subject to annual thawing and freezing in areas underlain by permafrost. Although "active layer" is a literal translation from the old Russian permafrost literature, contemporary Russian permafrost literature does not use it and distinguishes between (a) the seasonally thawed layer over permafrost, and (b) the seasonally frozen layer over unfrozen soil.

The depth of the active layer is measured at the end of summer with a permafrost probe or with a pit dug to the bottom of the active layer. The thickness of the active layer greatly depends on local conditions such as vegetation and soil composition. Local factors often have greater impact on the thickness of the active layer than do regional (climate) factors. In the continuous permafrost zone, the active layer freezes in the first part of a winter and its thickness is defined by summer factors. In the discontinuous permafrost zone, the maximum thickness of the active layer is limited by the thickness of the layer, which can become frozen during winter, and the thickness of the active layer as well as the permafrost's existence is defined by winter factors.

1.4 Factors Influence Permafrost Conditions

Many factors can influence permafrost conditions, basically changing its surface and internal temperatures. According to Jorgenson and Osterkamp (2009), the following factors can influence permafrost: climate (air temperature, rain, snow, wind); physical terrain (topography, slope, aspect); hydrology (surface drainage and set wetness, water bodies nearby, underground water); vegetation (shading, insulation,

snow interception); geology (soil and rock, geothermal heat flow, tectonic setting); and disturbances (human, animal, fire).

Although many factors can influence permafrost and its regional distribution, climate is one of the most important. Based on Ferrians (1994), Barrow, Alaska, has the lowest mean annual air temperature, -12.2°C. However, Anchorage has a mean annual air temperature of 1.7°C.

Air climate and permafrost climate are two different things. Based on my permafrost class course ware (Shur, 2014), air climate is the product of solar radiation and air circulation. Permafrost climate is not a simple derivative of the atmospheric climate, but a result of atmospheric climate's transformation by the soil surface and the active layer. Permafrost climate is also a product of those which modify the air climate. Modifiers might be relief, vegetation, snow, and surface water.

The effectiveness of modifiers depends on their properties and the climatic conditions. Modifiers can reduce the depth of active layer. In some climate conditions, the permafrost's very existence depends on modifiers.

Shur and Ping (1994) divided all climates into three types for permafrost: (1) Climate sufficient for permafrost formation (permafrost must exist); (2) Climate unfavorable to permafrost formation (permafrost cannot exist except under special conditions); and (3) Climate neutral to permafrost formation (permafrost can or cannot exist). In areas with a sufficient climate, permafrost forms everywhere under land and under shallow water. Climate modifiers like vegetation and relief influence the depth of the active layer and permafrost temperature. In areas with climate unfavorable to permafrost, permafrost local modifiers cannot sufficiently reduce soil temperature because of the warm climate. A climate neutral to permafrost is most interesting. In this case, permafrost forms or can exist only in terrain that has special combinations of snow cover, relief, vegetation, and soil. Modifiers in this case

determine permafrost existence, and a change of modifiers can lead to permafrost degradation or aggradation. Vegetation is an important modifiers. It usually has a cooling effect on soil. Among different types of vegetation, moss has the greatest impact: it can reduce soil temperature approximately 1 to 1.5°C. The most important factor for soil temperature is snow. It decreases soil heat-loss in winter. We need to distinguish between snow layer and snow-fall. Snow layer is a modifier, but snow fall is a component of climate. If the snow depth is equal to the critical depth, soil temperature at the bottom of the active layer is equal to 0°C. Another factor is critical depth of water, which makes mean annual soil temperature beneath it equal to 0°C. If the water depth is greater than the critical depth, a talik will develop beneath the water.

1.5 Thermal History of Permafrost in Alaska

The occurrence, distribution and thickness of permafrost increased during the last ice age. Most of the thick permafrost formed in the exposed continental shelves of the Arctic and Antarctic Oceans. But since the global warming began 10,000 years ago, permafrost has been limited to polar and high mountain regions, and thick permafrost is thinning from the bottom.

The U.S. Geological Survey has measured temperatures in deep drill holes in permafrost in Northern Alaska since the 1940s. The results show a 2°C to 4°C increase in permafrost temperature. According to Osterkamp (2003), this warming began approximately about 40 to 80 years ago. Warming of the air temperature in the late 1800s and early 1900s in North America may be the reason for the warming of the permafrost. The discontinuous permafrost in Alaska has warmed along with the air temperature since the "little ice age" and the first thermokarst forming in the late 1880s. The continuous permafrost at Barrow has warmed since the late 1970s. At the 10m depth, measured results showed that the temperatures have risen about 1.5°C since 1976. "Permafrost remains stable and survives only because of the insulating effect of the organic mat at the surface and the related thermal offset in the active

layer".

Figure 3 clearly shows the temperature increase in different places at 20m depth since the late 1970s.

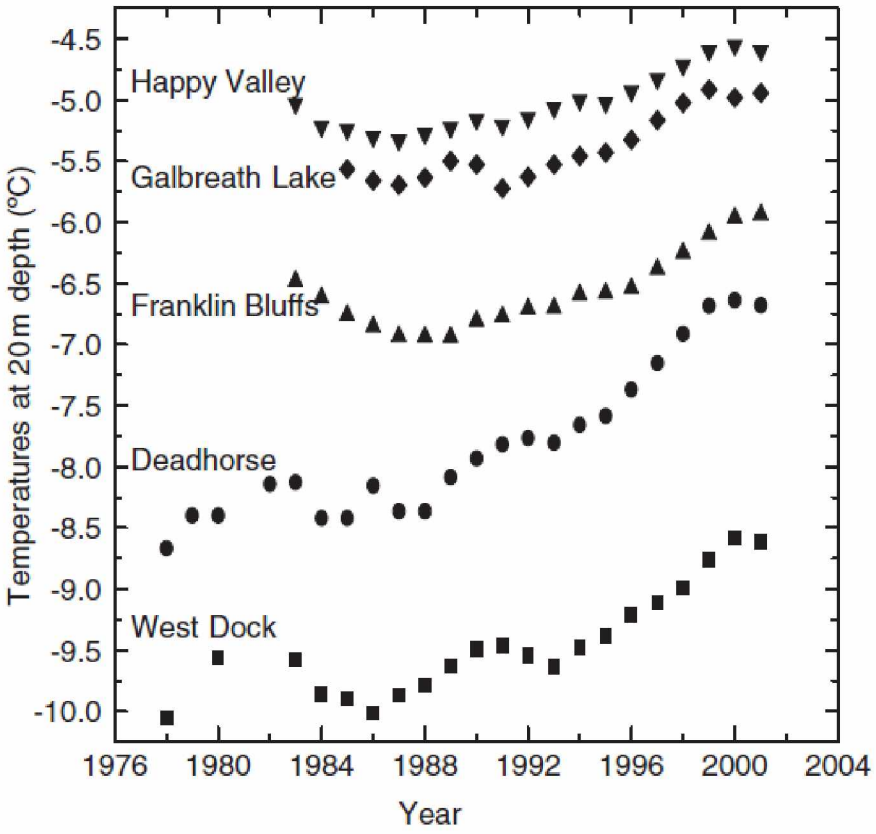

Figure 3. Time series of temperatures at the 20m depth for sites from Prudhoe Bay south to the Brooks Range in Alaska (Osterkamp 2003)

We focus on the thermal history because any changes in permafrost temperature will cause changes in permafrost conditions. From Osterkamp's paper (2003), the first change is the thawing of isolated permafrost bodies. Any warming of the temperature will change the energy balance and cause thawing at the boundaries of permafrost bodies in the discontinuous permafrost. The second change caused by warming is thermokarst. Thermokarst forms when ice-rich permafrost thaws. This process can disrupt ecosystems, human activities, infrastructure, and energy fluxes. The third change is basal thawing. The temperature increases at the surface of the permafrost penetrates to the base side of it. This warming then could cause basal thawing of thin discontinuous permafrost.

1.6 Wellbore Instability

Wellbore instability is one of the most serious problems that engineers may encounter during the drilling operation. Wellbore instability can take several forms: (1) Caving shale or hard rock spalling may cause the wellbore enlargement; (2) If the wellbore fluid pressure is too high, fracturing of the formation may result; (3) If the pressure is too low, the hole could collapse.

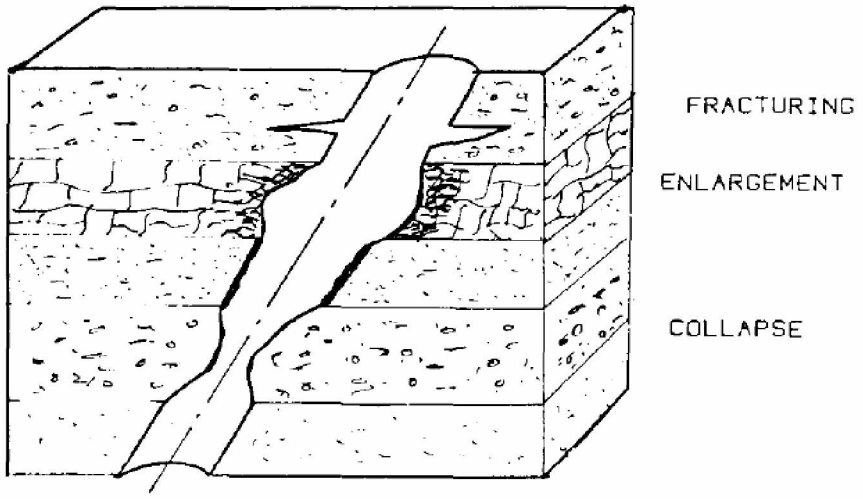

Figure 4. Types of Wellbore Instability (Cheatham, 1984)

1.6.1 Causes of Wellbore Instability

The causes of wellbore instability are often mechanical and/or chemical. Cheatham (1984), gave these reasons for wellbore instability: (1) Hydration swelling of shale, resulting in caving and hole enlargement used to be one of the most significant causes. But as drilling fluids performance developed, the effect of hydration swelling of shale have been reduced; (2) Excessive wellbore pressure can cause lost circulation; (3) Excessive production rates can cause solid-particle influx and hole enlargement; and (4) Low wellbore pressure can cause a blowout or hole collapse.

Wellbore stability is usually caused by a combination of different factors, controllable and uncontrollable. Table 1 from Pašić et.al. (2007) shows controllable and uncontrollable causes of wellbore instability.

Table 1: Causes of Wellbore Instability (B. Pašić, 2007)

Uncontrollable (Natural) Factors	Controllable Factors
Naturally Fractured or Faulted Formations	Bottom Hole Pressure (Mud Density)
Tectonically Stressed Formations	Well Inclination and Azimuth
High In-situ Stresses	Transient Pore Pressures
Mobile Formations	Physical/chemical Rock-Fluid Interaction
Unconsolidated Formations	Drill String Vibrations
Naturally Over-Pressured Shale Collapse	Erosion
Induced Over-Pressured Shale Collapse	Temperature

1.6.2 Bottom-Hole Pressure

Well bottom-hole pressure, or in other words, the mud density of the drilling fluid, is the most important determinant of wellbore stability. Static or dynamic, the pressure of the fluid during drilling, stimulating, or producing can be used as support pressure to counteract the in situ stresses and pore pressure. This pressure will determine the stress concentration near the wellbore. As rock failure is dependent on the effective stress, the quicker the fluid pressure penetrates the wellbore wall, the more stable the well is. However, this does not mean the higher the mud densities or bottom hole pressures the better. For example, in fractured formations, a rise in bottom hole pressure may cause wellbore instability and compromise other criteria.

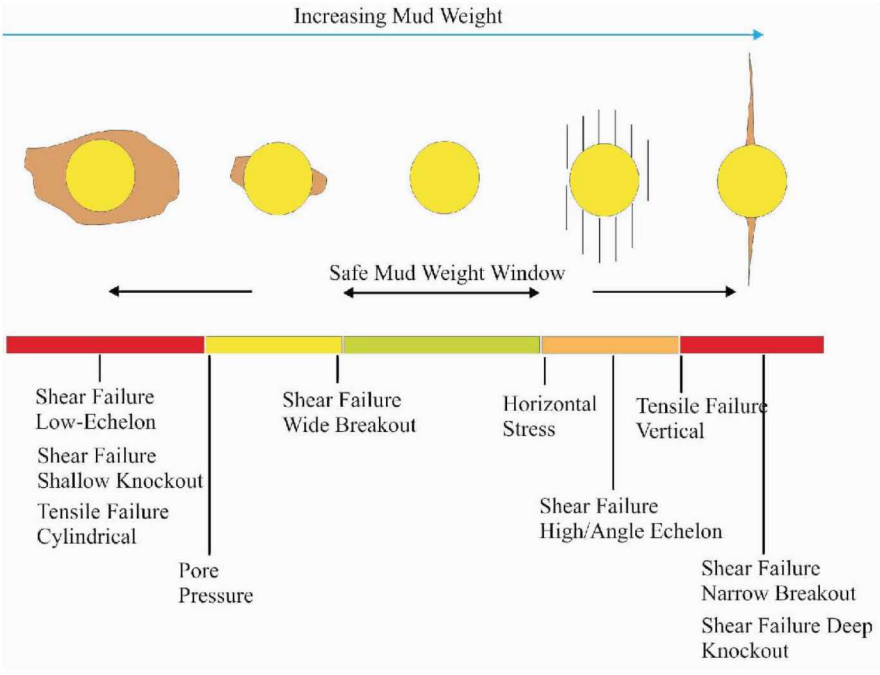

Figure 5. Effect of Mud Weight on Stress in Wellbore Wall (Pašić, 2007)

1.6.3 Wellbore Instability Indicators

Pašić et al. classified wellbore instability indicators into two groups: direct indicators and indirect indicators. All indicators are listed in Table 2.

Table 2: Indicators of Wellbore Instability (B. Pašić,2007)

Direct Indicators	Indirect Indicators
Oversize hole	High torque and drag (friction)
Undergauge hole	Hanging up of drillstring, casing, or coiled tubing
Excessive volume of cuttings	Increased circulating pressures
Excessive volume of cavings	Stuck pipe
Cavings at surface	Excessive drillstring vibrations
Hole fill after tripping	Drillstring failure
Excess cement volume required	Deviation control problems
	Inability to run logs
	Poor logging response
	Annular gas leakage due to poor cement job
	Keyhole seating
	Excessive doglegs

From caliper logs of the well, overgauge or undergauge holes can be observed. More cuttings and/or cavings from the gauge hole than would normally be expected from its excavation would signal hole enlargement. Spalling processes are occurring in the wellbore if cavings at the surface and hole fill after tripping occurred. Also, if the cement volume is larger than the calculated drill hole volume, the wellbore is enlarged.

1.7 Problems for Arctic Wells

According to Ferrians (1994), two basic methods are used for construction on permafrost: the active method and the passive method. The active method is used in areas with thin and discontinuous permafrost and where the permafrost contains relatively small amounts of ice. This method is to thaw the permafrost first and check if the thawed material has an available bearing strength. If it does, construction proceeds in a normal way. However, the passive method is to keep the permafrost

frozen. The passive method is used widely in the Interior and in northern Alaska where permafrost is widespread, thick and ice rich near the surface. For the passive method, engineers must avoid disturbing the permafrost at all cost. Many techniques could be used to keep permafrost frozen, like using different kinds of insulation, elevating heated structures above the ground surface, and using mechanical refrigeration.

For arctic well drilling, completion, and production, an engineer's main problem is dealing with permafrost thawing during these operations. According to Goodman (1978), the thaw radius during drilling for uninsulated wells at Prudhoe Bay and Mackenzie Delta could be 3 feet. Over twenty-year production, the thaw radius could reach 50 feet. The thaw radius depends on the thermal properties of permafrost, discussed later. Figure 6 is a typical thaw radius example at different times for a conventional production well in permafrost formation.

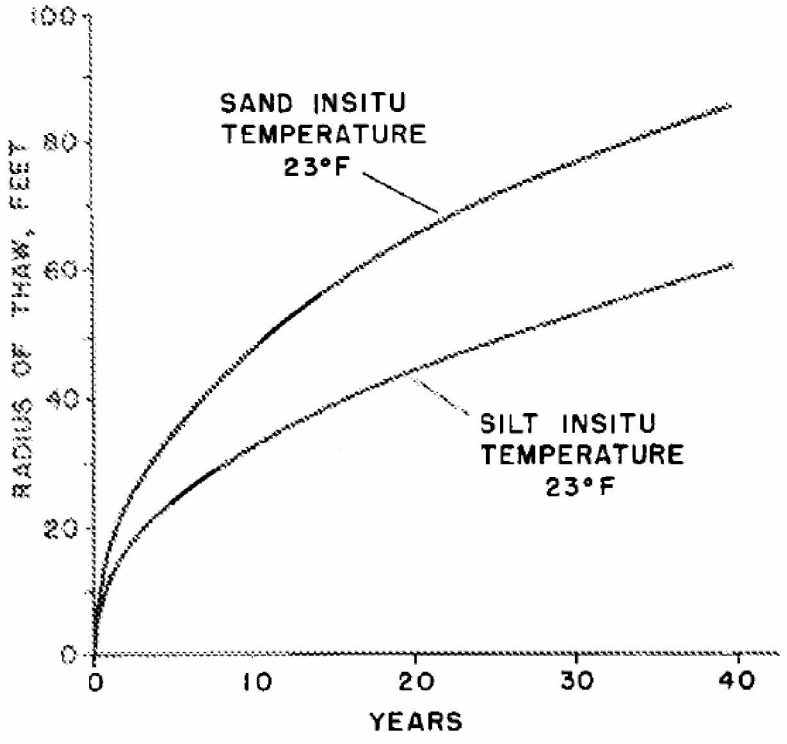

Figure 6. Radii of Thaw around a Conventional Production Well

(Smith and Clegg,1971)

1.7.1 Thaw Subsidence

According to Goodman (1978), four mechanisms of thaw subsidence are: (1) excess ice melting; (2) thaw-consolidation with fluid expulsion; (3) pore pressure reduction; and (4) stiffness reduction.

Of these four mechanisms, excess ice is the most difficult to assess in the field. If excess ice exists, it can be found at or near the surface. If melting, the volume of excess ice could decrease 9%, and the soil would compacts due to loss of support. Then the soil at the top would slump.

Figure 7 shows the schematic of the thaw-consolidation process. This mechanism requires ice-rich soil and the presence of excess ice. The process can cause compaction of the soil: during thaw, pressure in the thaw zone will exceed hydrostatic pressure, and the fluid will flow out of the thawed zone. This mechanism contains two parts of deformation: phase change contraction of excess ice, and consolidation with fluid expulsion

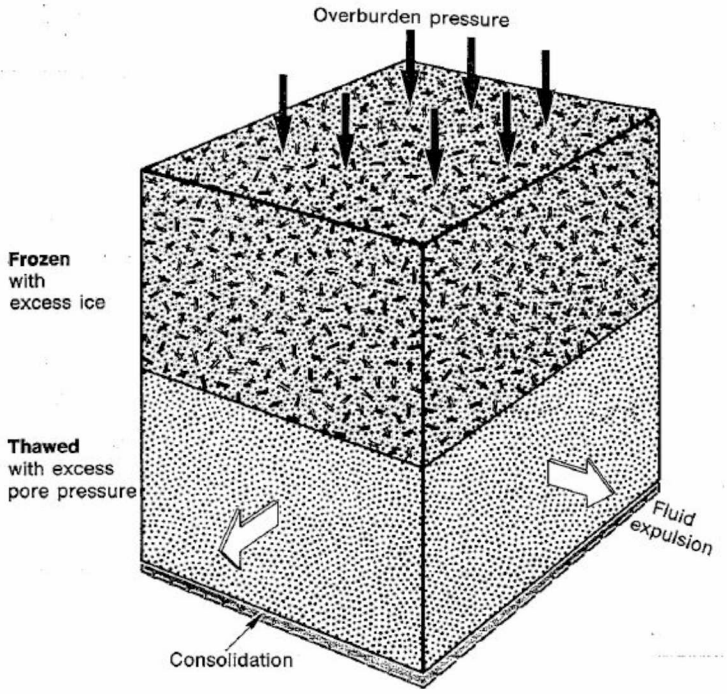

Figure 7. Schematic of Thaw-Consolidation Process (Goodman 1978)

The major mechanism of thaw subsidence in deep permafrost is pore pressure reduction. If the pore pressure in permafrost is decreases, the intergranular stress will increase and the soil will compact. Pore pressure reduction can be estimated by Equation 1.1, where Δp is the pore pressure reduction, ρ_i is formation density, z is depth and g is the gravitational constant:

$$\Delta p = \rho_i g z \quad \text{(Eq. 1.1)}$$

In this equation, the initial pressure before thaw is assumed to be hydrostatic and final pressure after thaw is zero.

Stiffness reduction is associated with a decrease in the soil's mechanical properties with thaw. Without support provided from the pore ice, the soil is softer and more easily to deform. From Goodman's paper (1978), the stiffness reduction in deep permafrost is in a relationship with the Young's modulus:

$$\frac{\Delta E}{E} \bar{\rho} g \quad \text{(Eq. 1.2)}$$

where ΔE is the change in modulus from frozen to thawed material and $\bar{\rho}$ is effective permafrost density, which is bulk density minus pore ice density.

As thaw subsidence changes the pore pressure and causes the soil to compact, the deep permafrost properties, thermal or mechanical, will change during the thaw. This may affect the stability of the wellbore. The drilling fluid, cement, and equipment used to control the wellbore's stability need to be carefully designed.

1.7.2 Internal and External Freezeback

According to Perkin's (1975), well bore casing damage in permafrost may result from two mechanisms, (1) refreezing of permafrost outside the casing (external freezeback); or (2) freezing of fluids in pipes (internal freezeback)

External freezeback means the refreezing of the water-based fluid outside the casing as the temperature changes. This always happens when the well is shut in or

after a short production period. The volume of the refrozen permafrost may not equal the volume of the permafrost previously thawed. The significance of external freezeback is that this process could generate inward radial loads around the wellbore. These extra loads may cause the hole to collapse and make the wellbore unstable.

Internal freezeback is the freezing of the annulus fluid between the inner and outer casing because of the outside permafrost's low temperature. This freezing of fluid could either burst the outer string or collapse the inner string. Early experience in Arctic cementing suggested that casing-casing annuli should not be cemented. In cases of internal freezeback, special field procedures for cement placement in Arctic regions are required. These procedures or requirements can be found in a lot of papers (Goodman 1978; Benge et.al. 1982).

1.7.3 Other Problems

As drilling in permafrost is different from drilling in normal formation, many problems can occur during operations. Engineers must be able to deal with many other problems such as hydrate decomposition, which can increase the pressure; hole sloughing during drilling, which can cause stuck pipes; or drilling through hydrates which can make the mud become highly gasified.

Permafrost near the surface is impacted by human activities such as construction of necessary oilfield facilities and transportation after production. For total well safety, many properties need to be considered in terms of permafrost and its surrounding environmental conditions.

Chapter 2: Stress and Strain around the Wellbore and in Frozen Soil

As stated by Brady and Brown (2006), the most widely used definition of rock mechanics first given by the US National Committee on Rock Mechanics in 1964, is offered:

> *Rock mechanics is the theoretical and applied science of the mechanical behavior of rock and rock masses; it is that branch of mechanics concerned with the response of rock and rock masses to the force fields of their physical environment.*

Rock mechanics is used in all stages of a well design. To prevent wellbore collapse or other problems, a clear understanding of the forces from drilling fluid and formation pressure is important.

2.1 Stress and Strain

In rock mechanics, stress and strain are two key elements. A simple description of stress is the force divided by the area of the force applied surface.

$$\sigma = \frac{Force}{Area} = \frac{F_n}{A} \quad \text{(Eq. 2.1)}$$

$$\tau = \frac{F_p}{A} \quad \text{(Eq. 2.2)}$$

where σ is the normal stress which is the decomposed stress perpendicular to the surface and τ is the shear stress which is the decomposed stress parallel to the surface. Figure 8 shows these two stresses. Normal stress may cause tensile or compressive failure, while shear stress may result in shear failure.

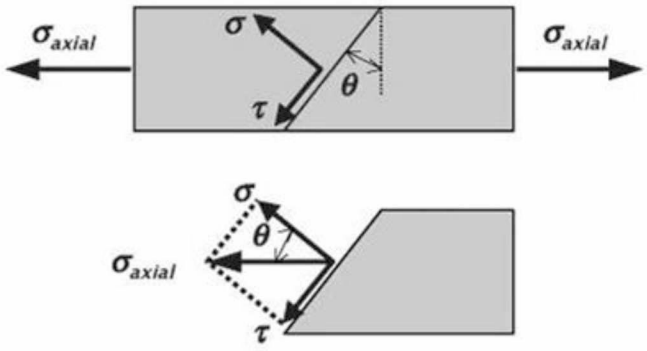

Figure 8. Stress Components of Normal and Shear Stress (Immerstein 2013)

Strain is a description of relative displacement of a point in a body under loading (**Figure 9**). The simple equation of strain ε is the deformed dimension Δl divided by the original state of the body l_0:

$$\varepsilon = \frac{\Delta l}{l_0} \quad \text{(Eq. 2.3)}$$

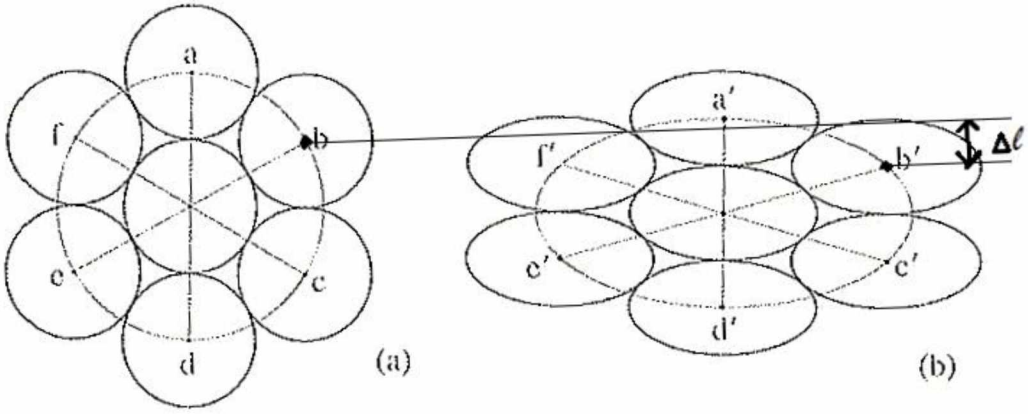

Figure 9. Center to Center distances: (a) Before Strain; (b) After Strain (Immerstein 2013)

When we look at a square under loading (Figure 10), the strain deformation can be classified into two parts: normal strain and shear strain. Examples of normal and shear strain equations can be found:

$$\varepsilon_{xx} = \frac{du_x}{dx} \quad \text{(Eq. 2.4)}$$

$$\gamma_{xy} = \frac{\pi}{2} - \beta = 2\alpha \quad \text{(Eq. 2.5)}$$

where ε_{xx} is the normal strain along x direction and γ_{xy} is the shear strain is the x, y plane. The displacement in x direction is du_x and dx is the length of the element. The deformation angle is α.

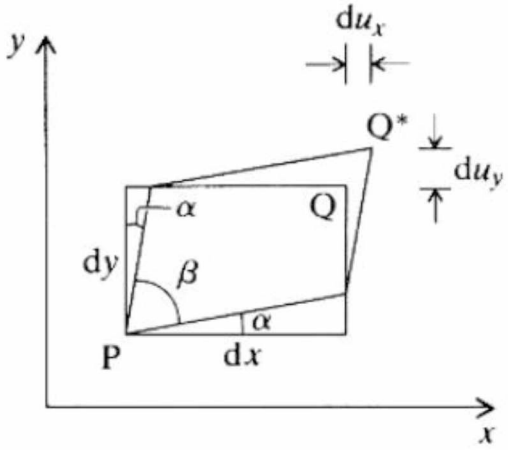

Figure 10. Displacement Produced by Normal and Shear Strain

(Brady and Brown 2004)

In some cases, stress and strain show a linear relationship also known as Hooke's law of deformation:

$$\sigma_x = E\varepsilon_x \quad \text{(Eq. 2.6)}$$

The slope of relationship E is the elastic modulus, better known as Young's modulus

2.2 **Principal Stress and In situ Stress**

When there are only normal stresses and no shear stresses on a given orientation, we could call these stresses principle stresses. Principal strains can be similarly defined as only normal strains on a given orientation and no shear strains. Principal stresses show the maximum differential stress value in a studied case. This is crucial in any failure analysis. According to Brady and Brown (2006), a cubic equation can be used to determine principal stresses:

$$\sigma_p^3 - I_1\sigma_p^2 + I_2\sigma_p - I_3 = 0 \quad \text{(Eq. 2.7)}$$

In this equation, I_1, I_2, and I_3 are called first, second and third stress invariants respectively. Expressions of them are:

$$I_1 = \sigma_{xx} + \sigma_{yy} + \sigma_{zz}$$

$$I_2 = \sigma_{xx}\sigma_{yy} + \sigma_{yy}\sigma_{zz} + \sigma_{zz}\sigma_{xx} - \left(\sigma_{xy}^2 + \sigma_{yz}^2 + \sigma_{zx}^2\right) \quad \text{(Eq. 2.8)}$$

$$I_3 = \sigma_{xx}\sigma_{yy}\sigma_{zz} + 2\sigma_{xy}\sigma_{yz}\sigma_{zx} - \left(\sigma_{xx}\sigma_{yz}^2 + \sigma_{yy}\sigma_{zx}^2 + \sigma_{zz}\sigma_{xy}^2\right)$$

Equation 2.7 produces three real solutions for the principal stresses, major principal stress (σ_1), intermediate principal stress (σ_2), and minor principal stress (σ_3) and $\sigma_1 > \sigma_2 > \sigma_3$.

In-situ stress can be classified into two main parts: vertical stress and horizontal stresses. Vertical stress of a point in the underground formations is the weight of the overlaying sediments of this point. It increases with depth and can be defined in a simple way as a function of formation density ρ, depth z, and gravity g as $\sigma_v = \rho g z$.

In rock mechanics, two values of horizontal stresses are always significant: maximum horizontal stress and minimum horizontal stress. In an isotropic formation, these two horizontal stresses will be equal to each other. Figure 11 is a schematic of in situ stress.

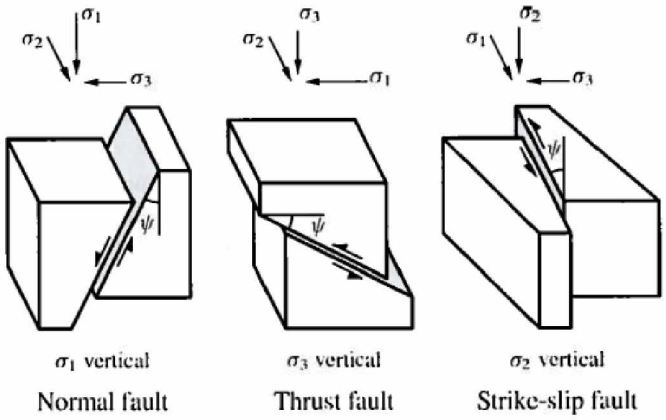

Figure 11. Schematic In situ Stress and Associated Fault Types (Immerstein 2013)

2.3 **Stresses around the Wellbore**

The initial state of stress in a formation will be changed after a well is drilled. Stresses around the wellbore can be defined by using Hooke's law, equilibrium equations and compatibility equations. Figure 12 is the schematic of stresses around a vertical well, Sx and Sy are maximum and minimum horizontal stresses and Sz is the

vertical stress

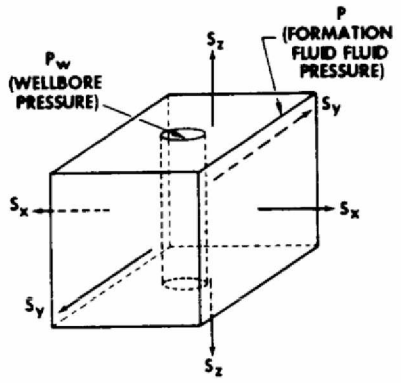

Figure 12. Schematic of Stresses Around a Vertical Well

(Deily and Owens 1969)

Jin and Chen (2012) summarized functions of stresses around a wellbore that was loaded with anisotropic horizontal stresses and vertical stress. This function is the well-known Kirsch equation:

$$\sigma_r = \frac{R^2}{r^2}p_i + \frac{\sigma_{xx}+\sigma_{yy}}{2}\left(1-\frac{R^2}{r^2}\right) + \frac{\sigma_{xx}-\sigma_{yy}}{2}\left(1+\frac{3R^4}{r^4}-\frac{4R^2}{r^2}\right)\cos 2\theta + \tau_{xy}\left(1+\frac{3R^4}{r^4}-\frac{4R^2}{r^2}\right)sin2\theta \quad \text{(Eq.2.9)}$$

$$\sigma_\theta = -\frac{R^2}{r^2}p_i + \frac{\sigma_{xx}+\sigma_{yy}}{2}\left(1+\frac{R^2}{r^2}\right) - \frac{\sigma_{xx}-\sigma_{yy}}{2}\left(1+\frac{3R^4}{r^4}\right)\cos 2\theta - \tau_{xy}\left(1+\frac{3R^4}{r^4}\right)sin2\theta \quad \text{(Eq.2.10)}$$

$$\tau_{r\theta} = \frac{\sigma_{xx}-\sigma_{yy}}{2}\left(1-\frac{3R^4}{r^4}+\frac{2R^2}{r^2}\right)sin2\theta + \tau_{xy}\left(1-\frac{3R^4}{r^4}+\frac{2R^2}{r^2}\right)cos2\theta \quad \text{(Eq. 2.11)}$$

In these equations, σ_r is the radial stress, σ_θ is the tangential stress, $\tau_{r\theta}$ is the shear stress, σ_{xx} and σ_{yy} are normal stresses, τ_{xy} is the shear stress applied on the boundaries, R is the wellbore radius and r is the distance from the center of the wellbore, p_i is the pressure in the wellbore, θ is the angle from the direction of the maximum principal stress.

For stresses on the wall of a wellbore, we could say that the distance from the center of the well is equal to the wellbore radius ($R = r$). Then the equations above reduce to:

$$\sigma_r = p_i$$

$$\sigma_\theta = -p_i + \sigma_{xx} + \sigma_{yy} - 2(\sigma_{xx} - \sigma_{yy})cos2\theta - 4\tau_{xy}\, sin2\theta \quad \text{(Eq. 2.12)}$$

$$\tau_{r\theta} = 0$$

2.4 **Creep of Frozen Soil**

Creep is the slow deformation of soil under constant stress. For step loading under uniaxial stress conditions and constant temperature, the creep type in Figure 13-(a) can be obtained. It is common for frozen soils and a large number of other materials. Figure 13-(b) shows the corresponding creep rate versus time plot. Three stages of creep show on the plot: (I) is primary creep with a decreasing rate of deformation; (II) is secondary creep with a constant rate of deformation; and (III) is tertiary creep with an increasing rate of deformation. If stresses of frozen soil are lower than the long-term strength, which is the maximum stress that the frozen soil can withstand indefinitely and exhibit either zero or continuously decreasing strain rate with time, the secondary and tertiary stages may not develop.

The magnitude of applied stress is not the only thing that can influence the shape of creep curves of frozen soils. Soil type, temperature, and density are also important. For example, the creep curve of Figure 13 (a) and (b) show the creep behavior of medium to high density ice saturated sands and silts. Ladanyi summarized a unified plot of creep data which is significant for creep of frozen soils (Figure 14).

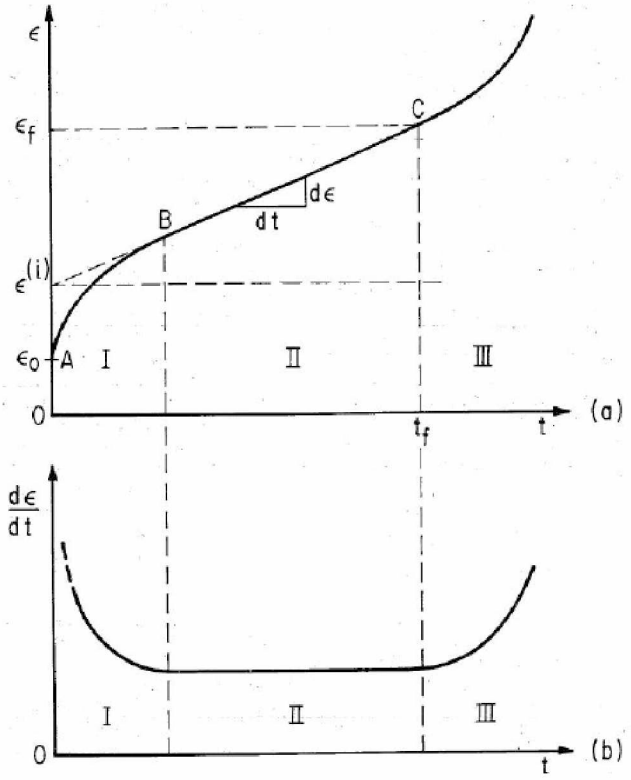

Figure 13. Stress and Strain in Constant Stress Creep Test (Landanyi 1972)

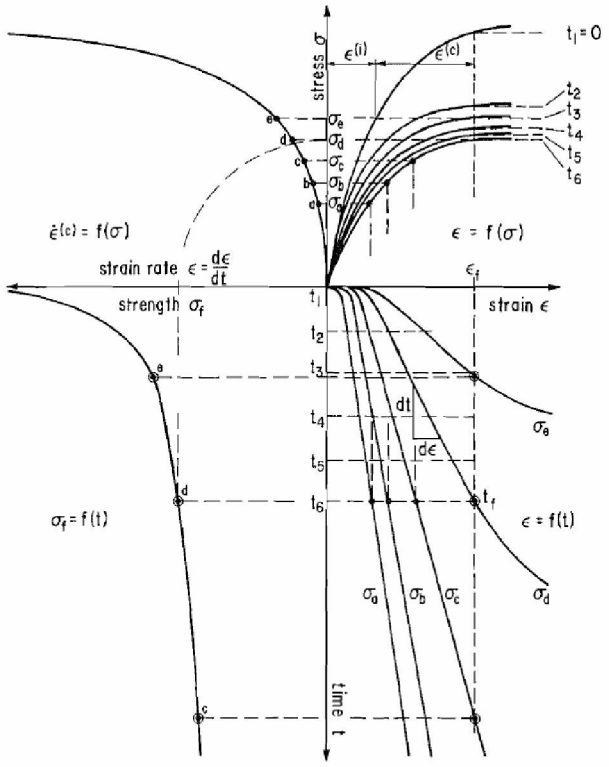

Figure 14. Schematic Plots of Data from Compression Creep Tests Conducted at Constant Temperature and Confining Pressure (Ladanyi 1972)

Chapter 3: Properties of Permafrost

Permafrost is a complex, multiphase system. According to Yuri Shur(2014), four components can be found in permafrost and each has different physical, mechanical, and thermal properties. The four components are: soil particles, ice, water, and air. Ice is the most important component and is a visco-plastic substance. It has three types: pore ice, ice inclusions, and massive ice.

3.1 Water Content

The total water content of frozen soil includes unfrozen water content; water content due to pore ice, in other words ice cement; and water due to ice inclusions. Engineers do not consider massive ice to determine the water content of frozen soil. The expression of water content can be written as:

$$W = W_{unfrozen} + W_{pore\ ice} + W_{inclusions} \quad \text{(Eq.3.1)}$$

All water contents are expressed as a ratio of the weight of water to the weight of dry soil. If there is no visible ice inclusion in the frozen soil, or we want to get the water content of frozen soils between ice inclusions, that means the $W_{inclusions}$ is equal to zero, and then the expression can be reduced to:

$$W = W_{unfrozen} + W_{pore\ ice} \quad \text{(Eq. 3.2)}$$

Water content of permafrost is important. The value of water content can be used to calculate bulk unit weight of soil, thermal conductivity, heat capacity, latent heat, and so on.

3.2 Cohesion

Cohesion is the cohesive forces that are acting between atoms. It is the ability of molecules to remain connected. In permafrost, according to Andersland and Ladanyi (2004), cohesion of frozen soil is related to uniaxial compression strength (UCS), the expression of which is:

$$c = \frac{UCS}{2N_{\varphi}^{0.5}} \quad \text{(Eq. 3.3)}$$

where c is cohesion, and N_{φ} is called flow value and is a function of friction angle

φ.

$$N_{\varphi} = \frac{1+\sin\varphi}{1-\sin\varphi} \quad \text{(Eq. 3.4)}$$

The UCS value of permafrost depends on soil type and temperature, so cohesion of permafrost is also temperature dependent. Figure 15 shows the UCS of different materials for temperature below 0°C.After reading values from the plot (Figure 15) and based on friction angle of different materials, we can calculate cohesion of different frozen soil. Cohesion for this simulation discussed in Section 4.1

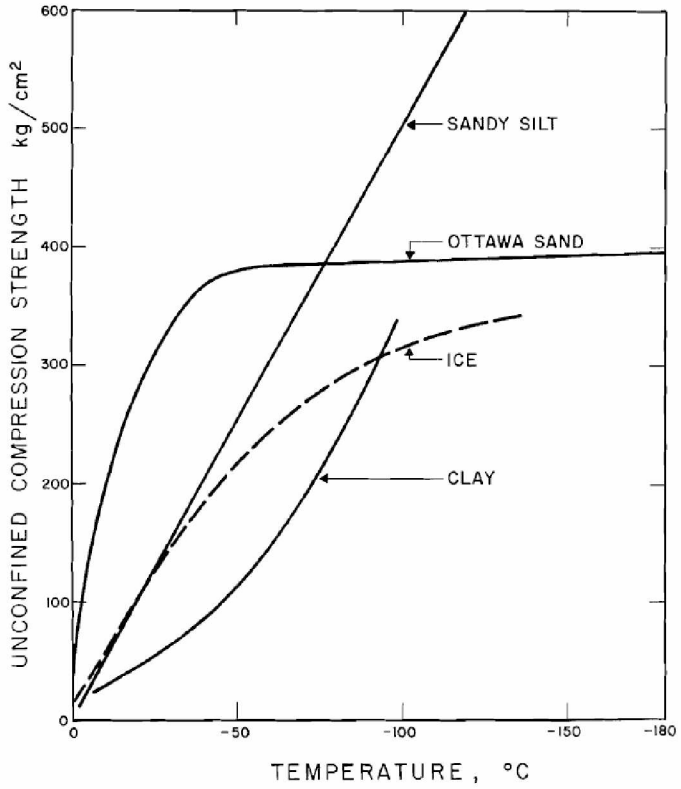

Figure 15. Temperature Dependence of UCS for Various Frozen Materials (Ladanyi 1972)

3.3 Young's Modulus

Young's modulus, also known as elastic modulus, measures the force that is needed to stretch or compress a material sample. Temperature change can strongly effect Young's modulus magnitudes. Young's modulus of frozen soil could be ten to hundreds of times higher than that of unfrozen soil.

From Andersland and Ladanyi's book (2004), cyclic compression tests on 200mm cubes of three different frozen soils were done by Tsytovich, the expressions of which follow:

For frozen sand:

$$E = 500(1 + 4.2\theta) \quad \text{(Eq. 3.5)}$$

For frozen silt:

$$E = 400(1 + 3.5\theta) \quad \text{(Eq. 3.6)}$$

For frozen clay:

$$E = 500(1 + 0.46\theta) \quad \text{(Eq. 3.7)}$$

In all these functions, θ is the absolute value of temperature below 0°C and E is Young's modulus in MPa.

3.4 Volumetric Heat Capacity and Latent Heat of Fusion

Volumetric heat capacity is the quantity of heat required to change the temperature of a unit volume by 1degree. Expressions of heat capacity for frozen and unfrozen soil are as follows:

For unfrozen soil:

$$C_u = \gamma_d \left(c + \frac{1.0W}{100}\right) \quad \text{(Eq. 3.8)}$$

For frozen soil:

$$C_{fr} = \gamma_d \left(c + \frac{0.5W}{100}\right) \quad \text{(Eq. 3.9)}$$

where capital C is heat capacity in BTU/ft^3°F; c is specific heat of soils, for mineral soil c equals 0.17 Btu/lb°F; The soil dry density is γ_d; and W is water content in percentage (Shur, 2014).

Volumetric latent heat of fusion can be defined as the quantity of heat required to melt the ice (or freeze the water) in a unit volume of soil without a change in temperature. It is also a function of water content of soil. The expression for latent heat is:

$$L = \rho\gamma_d \left(\frac{W}{100}\right) \quad \text{(Eq. 3.10)}$$

The latent heat in Btu/ft^3 is L, and ρ is the mass latent heat for water that equals 144 Btu/lb, so the function can be written as:

$$L = 144\gamma_d \left(\frac{W}{100}\right) \quad \text{(Eq. 3.11)}$$

Figure 16 is a schematic of heat capacity and latent heat, where x-axis is the temperature and y-axis is the quantity of heat.

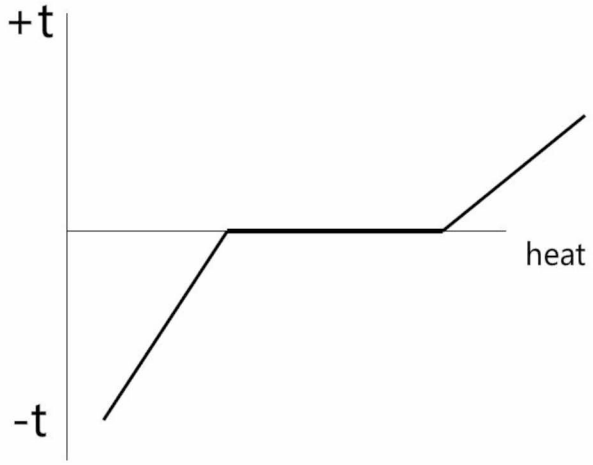

Figure 16. Schematic of Heat Capacity and Latent Heat (Shur 2014)

3.5 Thermal Conductivity

Thermal conductivity is one of the most important parameters of permafrost. It shows the property of a material to conduct heat. If the soil's dry density and its degree of saturation increases, the amount of heat transferred by conduction in soil increases. Table 3 summarizes the thermal properties of selected materials

Table 3: Thermal Properties of Selected Materials

(Andersland and Ladanyi 2004)

Material	Density (kg/m3)	Heat Capacity (kJ/kg/°C)	Thermal Conductivity(W/m/K)
Air, 10°C	1.25	1.00	0.026
Water, 0°C	999.87	4.2177	0.56
10°C	999.73	4.1922	0.58
Ice, 0°C	900	2.09	2.21
-40°C	900	2.09	0.08
Snow, loose	85	2.09	0.08

compacted	500	2.09	0.7
Polystyrene, foam	30	1.25	0.035
Polyurethane, foam	32	1.67	0.024
Rock wool	160	0.84	0.039
Glass wool	64	0.84	0.042
Straw, compressed	360		0.09
Wood			
Plywood, dry	600	2.7	0.17
Fir or pine, dry	500	2.5	0.12
Maple or oak, dry	700	2.09	0.17
Concrete			
Sand and gravel aggregate	2,200	0.89	1.3-1.7
Lightweight aggregate	1,880		0.74
Concrete, asphalt	2,050-2,150		1.05-1.52
Quartz	2,660	0.733	8.4
Granite		0.8	1.7-4.0
Limestone	2,640		1.3-5.0
Shale			1.5
Sandstone			1.8-4.2
Steel	7,500	0.5	43
Iron, ductile	7,500		51
Aluminum	2,700	0.88	156-190
Copper	8,950	0.42	386

However, values in Table 3 are representative. Most materials have some variation with density and temperature change. According to Andersland and Ladanyi (2004), Farouki summarized the following equations in SI units to calculate coarse-grained and fine-grained soil thermal conductivities:

For coarse-grained soil:

$$k_{un} = 0.1442(0.7 \log w + 0.4)(10)^{0.6243\rho_d} \quad \text{(Eq. 3.12)}$$

$$k_{fr} = 0.01096(10)^{0.8116\rho_d} + 0.00461(10)^{0.9115\rho_d} w \quad \text{(Eq.3.13)}$$

For fine-grained soil:

$$k_{un} = 0.1442(0.9 \log w - 0.2)(10)^{0.6243\rho_d} \quad \text{(Eq.3.14)}$$

$$k_{fr} = 0.001442(10)^{1.373\rho_d} + 0.01226(10)^{0.4994\rho_d} w \quad \text{(Eq.3.15)}$$

Unfrozen and frozen thermal conductivity in W/m/K are k_{un} and k_{fr}, respectively;

water content is w; and ρ_d is dry density in g/cm^3.

Compared with the thermal conductivity measured values; the calculation values from Equation 3.12 to 3.15 differ less than 25%. Hence average thermal conductivities are appropriate for most thermal problems, and reading thermal conductivity values from plots is easier and faster. Figure 17 (a) shows the average thermal conductivity for frozen sand and gravels; Figure 17 (b) is for unfrozen condition; Figure 18 (a) and (b) are average thermal conductivity for silt and clay soils under frozen and unfrozen conditions, respectively.

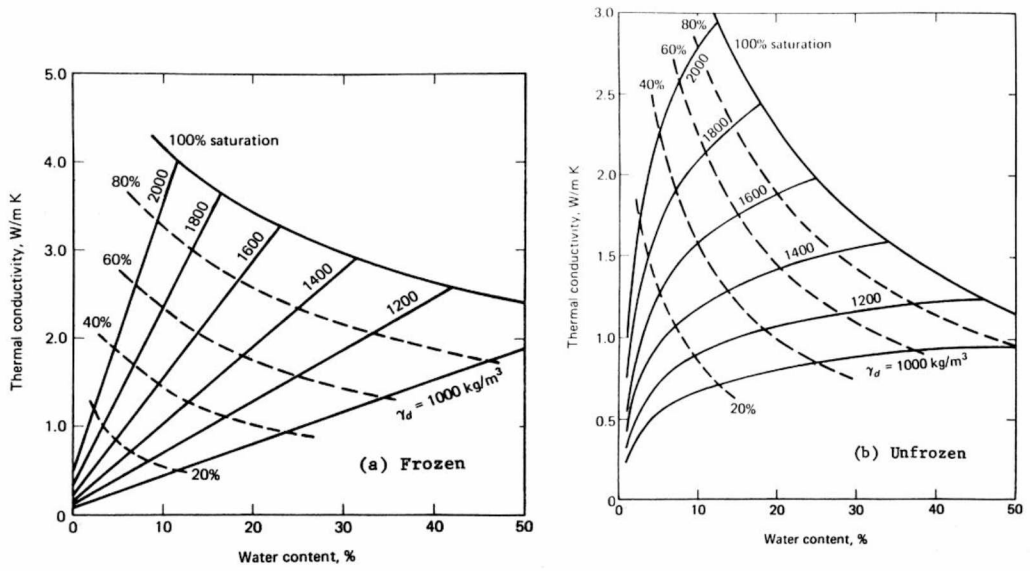

Figure 17. Average Thermal Conductivity for Sands and Gravels (Andersland and Ladanyi 2004)

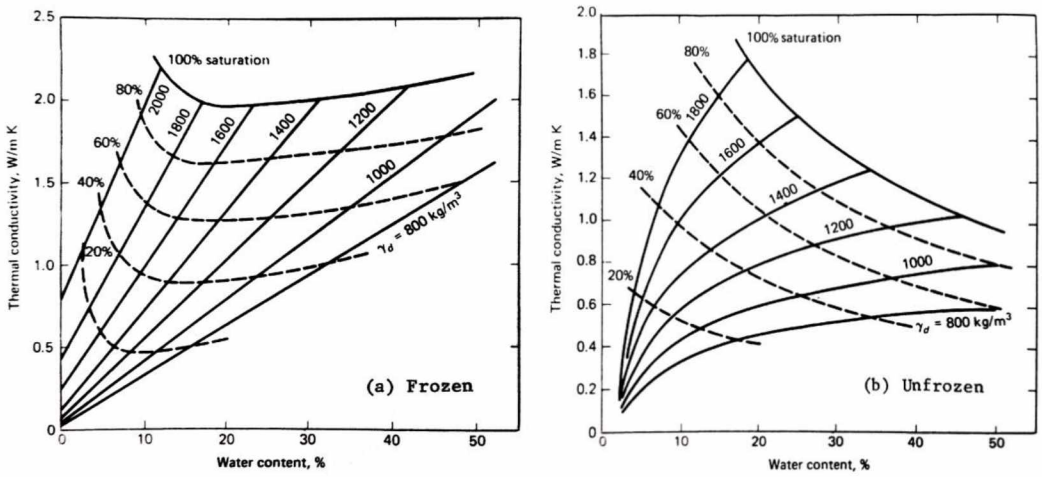

Figure 18 Average Thermal Conductivity for Silt and Clay

(Andersland and Ladanyi 2004)

Chapter 4: Simulation of a Vertical Well in Permafrost with FLAC

FLAC is short for "Fast Lagrangian Analysis of Continua". According to FLAC manual, Cundall first developed FLAC in 1986. It is a two-dimensional explicit finite difference program for engineering mechanics computation. From the product manual for FLAC issued by the Itasca Consulting Group, this program simulates the behavior of structures built of soil, rock, or other materials. The explicit, Lagrangian calculation scheme and the mixed-discretization zoning technique used in FLAC ensure that plastic collapse and flow are modeled very accurately.

A vertical well was simulated in the study. To minimize the influence of thawing permafrost on wellbore stability, the permafrost formation needs to be penetrated through the shortest distance. A vertical well is, therefore, the optimal choice of oil well development in permafrost formation.

To get the minimum wellbore stabile pressure as a function of temperature is the objective of this simulation. With the help of this expression, safety pressure for industry can be calculated before drilling. It could reduce the risk during operation and increase production.

4.1 Data Used in Simulation

Properties of permafrost used in this simulation were assumed as there were no real well data available when the simulation was run. The total depth of the permafrost formation in the simulation was 560 m, and was divided into three layers: clay (0m-120m), silt (120m-260m), and sand (260m-560m). The initial temperature of the permafrost in the model was set at -6°C, as most permafrost temperature is higher than -10°C.

From Ladanyi's paper (1972), one might expect to find the following values of friction angle for these three different materials: (1) Sands: φ=30°; (2) Silt: φ=20°;

and (3) Clay: φ=0-10°. So in the model the frictional angle of sand, silt, and clay were 30°, 20°, and 10° respectively.

Cohesions are calculated based on Equation 3.3 after friction angles were set. The UCS values are read from Figure 15. Figure 19 shows cohesions of different materials at negative temperature. Table 4 illustrates values of UCS and cohesion at different negative temperature for these three materials. For cohesion above 0°C,three constant values were used for these materials: sand is 1.26 MPa, silt is 0.26 MPa, and clay is 0.68 MPa. As tension strength value in the simulation, 1/8 of the UCS value was used based on Dan Luo's paper

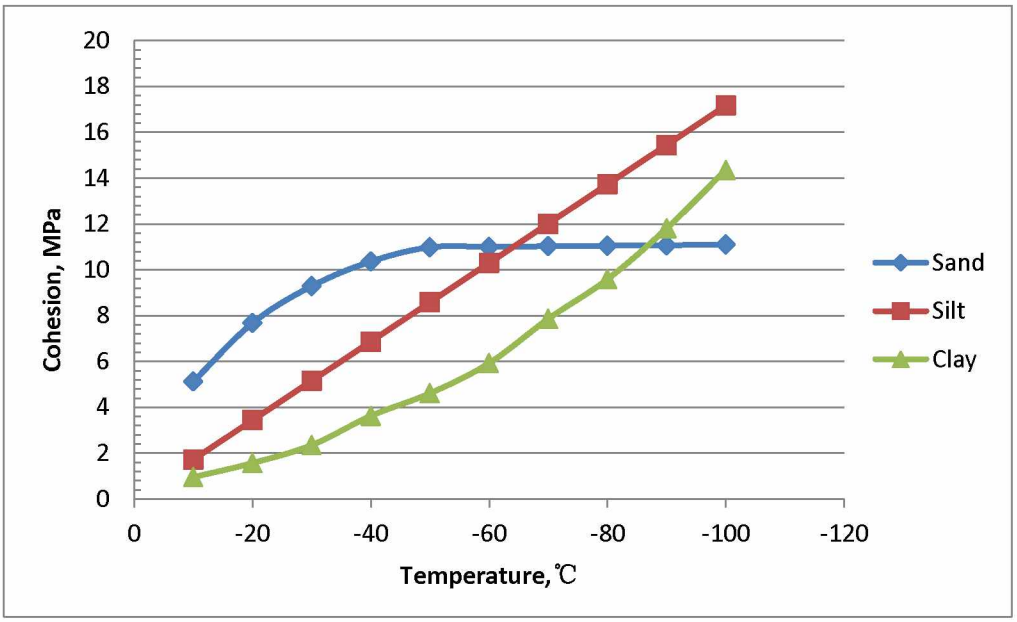

Figure 19. Cohesions of Different Materials at Negative Temperature

Table 4: UCS and Cohesion of Different Materials at Specific Friction Angle

	Sand		Silt		Clay	
Temperature	**UCS**	**Cohesion**	**UCS**	**Cohesion**	**UCS**	**Cohesion**
°C	**MPa**	**MPa**	**MPa**	**MPa**	**MPa**	**MPa**
-10	17.74	5.12	4.90	1.72	2.25	0.95
-20	26.56	7.67	9.80	3.43	3.72	1.56
-30	32.14	9.28	14.70	5.15	5.59	2.34
-40	35.87	10.35	19.60	6.86	8.62	3.62
-50	38.02	10.98	24.50	8.58	10.98	4.60
-60	38.10	11.00	29.40	10.29	14.11	5.92

-70	38.18	11.02	34.30	12.01	18.72	7.85
-80	38.26	11.04	39.20	13.72	22.83	9.58
-90	38.34	11.07	44.10	15.44	28.13	11.80
-100	38.42	11.09	49.00	17.16	34.20	14.35

As mentioned in Section 3.3, the difference in Young's modulus values between frozen and unfrozen soils can be 10 to 100 times. In this simulation, 100 times difference is taken for Young's modulus of frozen and unfrozen soil as other times like 10 and 50 were not available to get the result pressure. To reduce the simulation time and work in an easy way, each material only has two values of Young's modulus: one for temperature below 0°C, which can be calculated from Equation 3.5 to 3.7, another one is Young's modulus under unfrozen condition, which is 100 times smaller than the Young's modulus under frozen condition. With initial temperature set to -6°C, Table 5 shows initial Young's modulus used for this simulation.

Table 5: Young's modulus of Different Materials under Frozen and Unfrozen Condition

	Young's Modulus (MPa)		
	Sand	**Silt**	**Clay**
Frozen	13100	8800	1880
Unfrozen	131	88	18.8

In situ stresses and pore pressure gradient used in this simulation were from McLellan's paper, vertical stress is 0.0201 MPa/m, horizontal stress is 0.0147 MPa/m, and pore pressure is 0.0102 MPa/m. Since only a horizontal 2D plane-strain model with top-view model built for the analysis, there was no additional vertical stress applied in the simulation. In the simulation permafrost is assumed to be an isotropic material, the maximum (Syy) and minimum (Sxx) horizontal stresses are, therefore, considered equal. In the simulation, reasonable wellbore pressures were tested every 20 meters, so values of Sxx, Syy, and pore pressure at each depth were listed in Table 6.

Table 6: Horizontal Stresses and Pore Pressure for the Simulation

	Depth	Sxx	Syy	Pore Pressure
	m	MPa	MPa	MPa
Clay	20	0.29	0.29	0.20
	40	0.59	0.59	0.41
	60	0.88	0.88	0.61
	80	1.18	1.18	0.82
	100	1.47	1.47	1.02
	120	1.76	1.76	1.22
Silt	120	1.76	1.76	1.22
	140	2.06	2.06	1.43
	160	2.35	2.35	1.63
	180	2.65	2.65	1.84
	200	2.94	2.94	2.04
	220	3.23	3.23	2.24
	240	3.53	3.53	2.45
	260	3.82	3.82	2.65
Sand	260	3.82	3.82	2.65
	280	4.12	4.12	2.86
	300	4.41	4.41	3.06
	320	4.70	4.70	3.26
	340	5.00	5.00	3.47
	360	5.29	5.29	3.67
	380	5.59	5.59	3.88
	400	5.88	5.88	4.08
	420	6.17	6.17	4.28
	440	6.47	6.47	4.49
	460	6.76	6.76	4.69
	480	7.06	7.06	4.90
	500	7.35	7.35	5.10
	520	7.64	7.64	5.30
	540	7.94	7.94	5.51
	560	8.23	8.23	5.71

In FLAC, the water content and latent heat cannot be directly entered into the model. The only way in FLAC to include the parameter of water content is by varying the thermal conductivity value of soil as a function of its water content. Densities of sand, silt, and clay in this simulation were 2100 kg/m^3, 2000 kg/m^3, and 1900 kg/m^3, respectively. Densities were assumed according to FLAC database. Based on Figure

17 and 18, frozen and unfrozen thermal conductivities of these three materials used in the simulation were assumed. They are listed in Table 7. In the simulation, large specific values from 272 K to 274 K were used to account for latent heat of permafrost at its melting point. Table 8 is the summary of parameters used for the initial mechanical analysis.

Table 7: Frozen and Unfrozen Thermal Conductivity of Different Materials

	Thermal Conductivity (W/m/K)		
	Sand	**Silt**	**Clay**
Frozen	2.21	1.96	1.24
Unfrozen	1.57	1.47	1.00

Table 8: Input Parameters for Initial Mechanical Analysis

	Density	**Friction Angle**	**Cohesion**	**Tension**	**Young's Modulus**	**Poisson's Ratio**
	kg/m^3	**degree**	**MPa**	**MPa**	**GPa**	
Sand	2100	30	3.75	1.62	13.1	0.3
Silt	2000	20	1.03	0.37	8.8	0.3
Clay	1900	10	0.85	0.25	1.88	0.3

4.2 Simulation Procedures and Model Construction

Procedures for this simulation can be summarized as follows: the first step is model establishment, which requires a basic understanding of FLAC and the model to be built; the second step is data preparation, already mentioned in Section 4.1; the third step is construction of a large 60-meter model to estimate thermal effect; in the fourth step, a 10-meter small model was built for stress and strain analysis. After the results were recorded, the simulation was repeated for a different depth.

As previously mentioned, horizontal section models with vertical top-view were built for sand, silt, and clay. The radius of the wellbore was 0.15m, the total depth of the permafrost formation was 560m, and simulation was repeated every 20 meters. All properties needed for the simulation can be found in Chapter 4.1.

A large 60-meter model was firstly built to estimate thermal boundary effect. This step is important because as well production proceeds, the permafrost formation temperature will change, so the fixed boundary temperature for the small model in FLAC does not always equal initial temperature of -6°C. For example, assuming that the thermal time was 1 year, from the large model, temperature at 10 meters after 1 year for sand was 270°K. Then this temperature value was used as the small model boundary temperature at 1 year thermal time instead of 267°K (-6°C). The boundary temperature from the large model is an estimation value because as the model is 60 meters wide, a 0.15m radius wellbore could be taken as a point on the plot. The value may not exact but it is fair enough for this simulation. Fluid temperature in the wellbore was assumed to be 343°K. The plots in Figure 20 to 22 are examples of temperature distribution of sand, silt, and clay at 1 year and 5 years of thermal time for the 60-meter large model.

For the next step, a 10-meter model was used to perform detailed in-situ stress analysis. Ten meters was chosen as the model size because the model width needed to be at least 6 times larger than the wellbore radius to minimize boundary effect. 0.9 meter width (6 times of 0.15 meters) was first tested as the model zone. However, this width was too small and the boundary temperature would reach above 0°C in a short period (less than one day). As mentioned before, formation properties, such as cohesion, Young's modulus, and thermal conductivity will remain as constant in unfrozen condition. If all properties were constant, the tested pressure would only change with depth and cannot show the effect of temperature on permafrost formation. After increase the model width to 10 meters, the thermal time could be increased to approximately 5 years. That is the reason why simulation model width is 10 meters. If no occurrence of failure around the well after pressure applied, tested minimum wellbore pressure at 1 week, 1 month, 1 year, and 5 years were recorded.

For example, in a frozen sand formation at depth of 440m with a thermal time of

one week, after 2.4 MPa was applied around the wellbore, no failure showed up in the graph (Figure 23). If the wellbore pressure was reduced to 2.3 MPa, then collapse would happen and yield would show on the state graph (Figure 24). To maintain wellbore stability, 2.4 MPa was the tested minimum wellbore pressure.

Simulation steps were repeated for clay at depth ranging from 0m to120m; silt from 120m to 260m; and sand from 260m to 560m. Results were recorded and presented in Chapter 5.

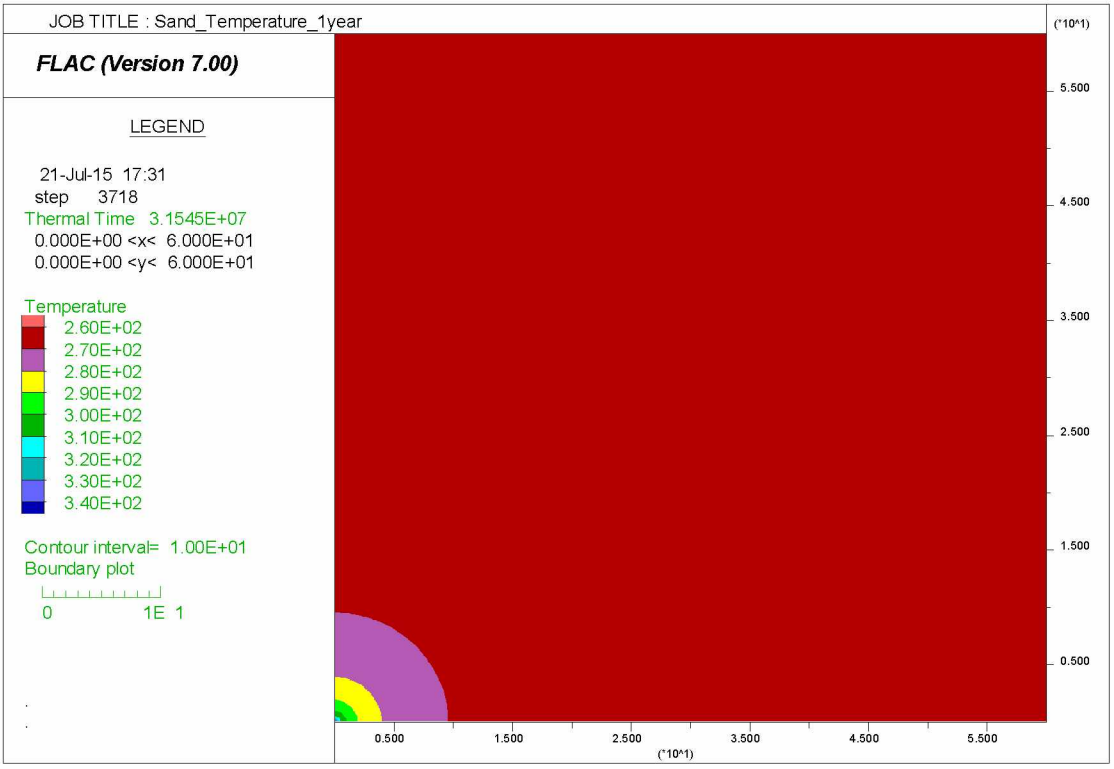

(a)

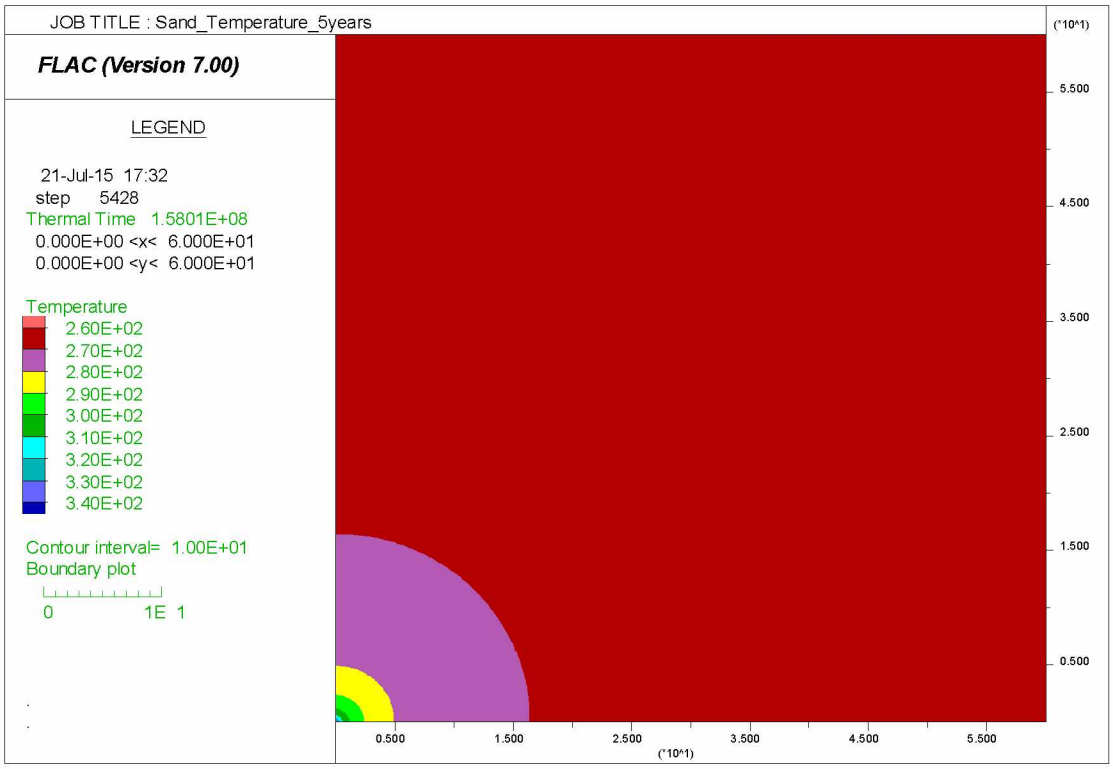

(b)

Figure 20. Temperature Distribution of Sand (a) 1year, thaw radius is 7.94 meters (b) 5 years, thaw radius is 10 meters

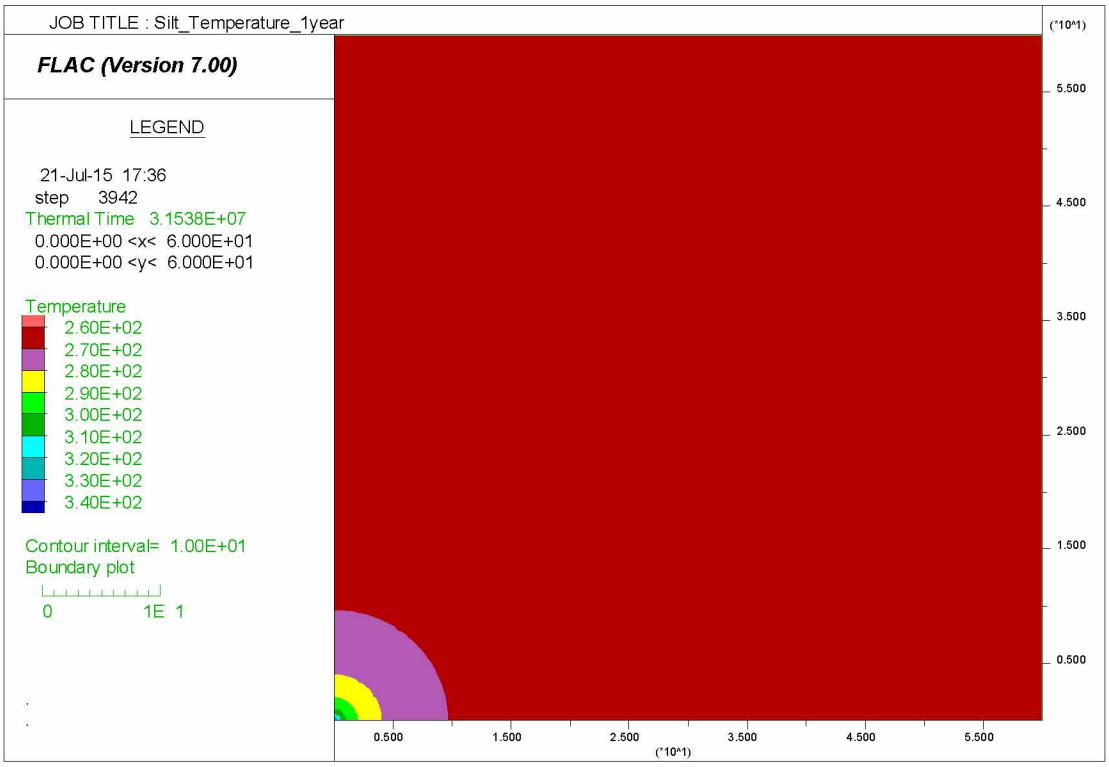

(a)

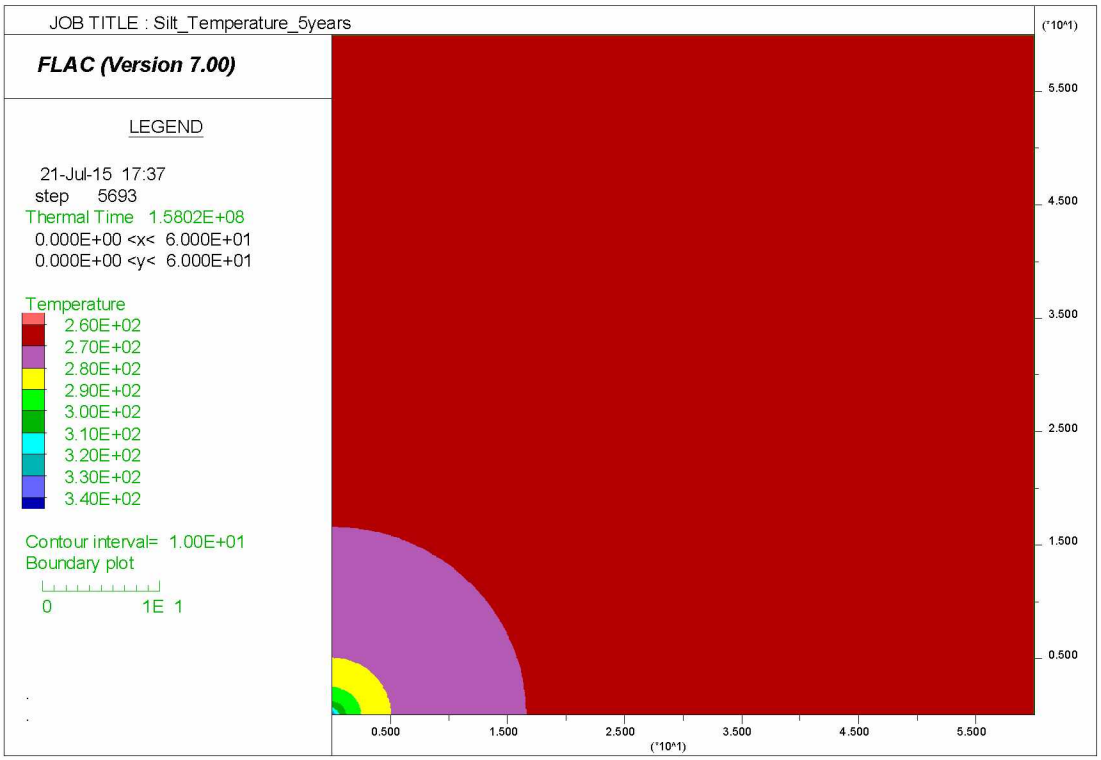

(b)

Figure 21. Temperature Distribution of Silt (a) 1 year, thaw radius is 8 meters (b) 5 years, thaw radius is 10 meters

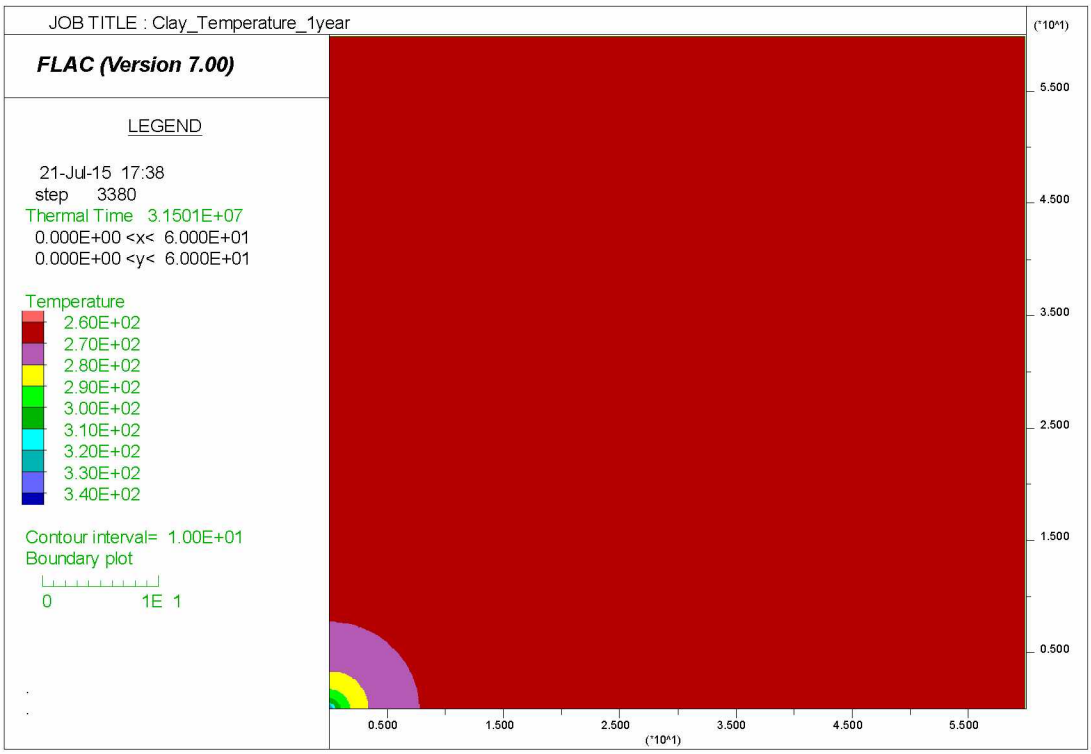

(a)

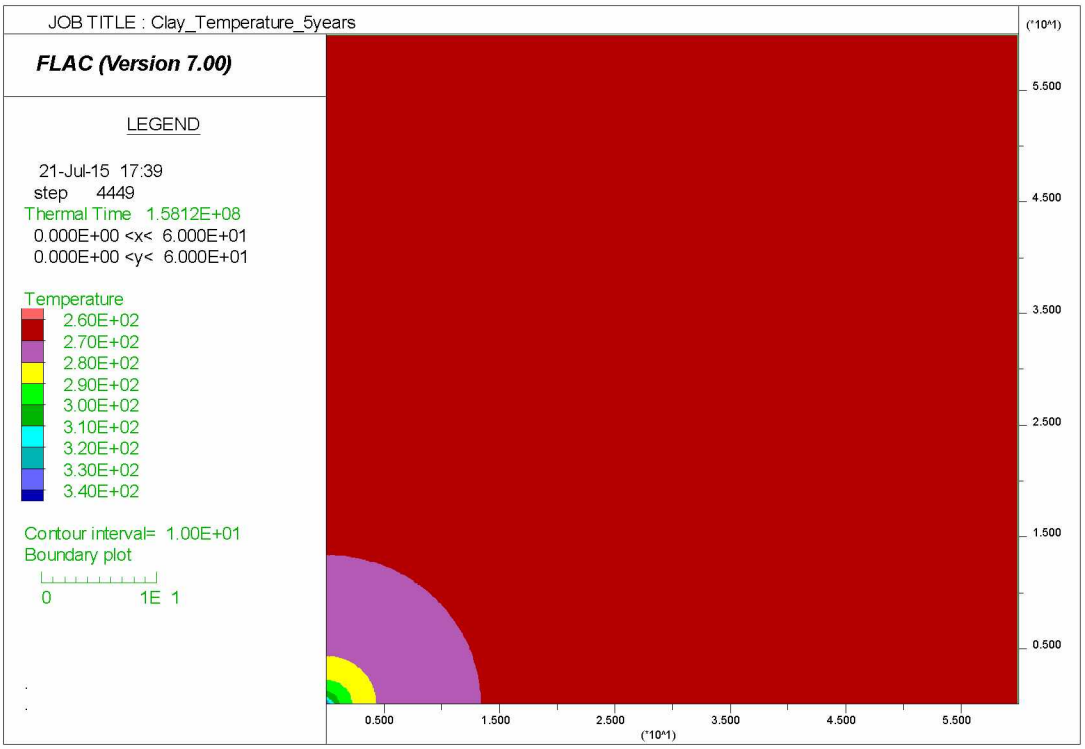

(b)

Figure 22. Temperature Distribution of Clay (a) 1 year, thaw radius is 6.6 meters (b) 5 years, thaw radius is 10 meters

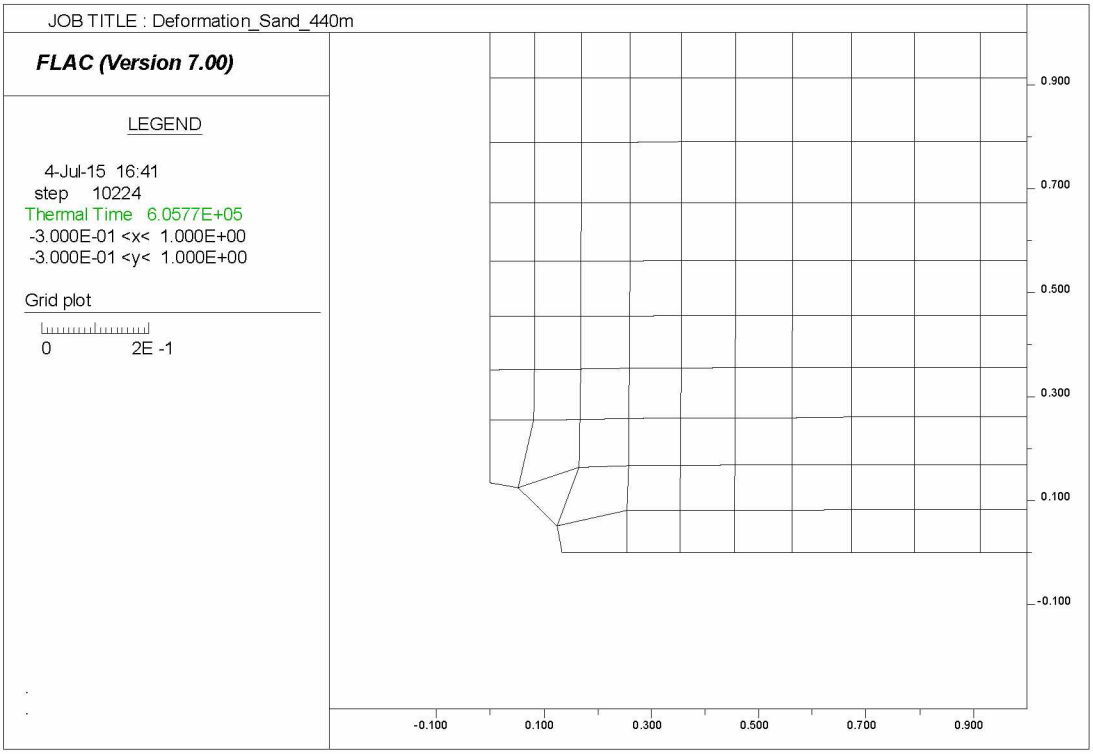

(a)

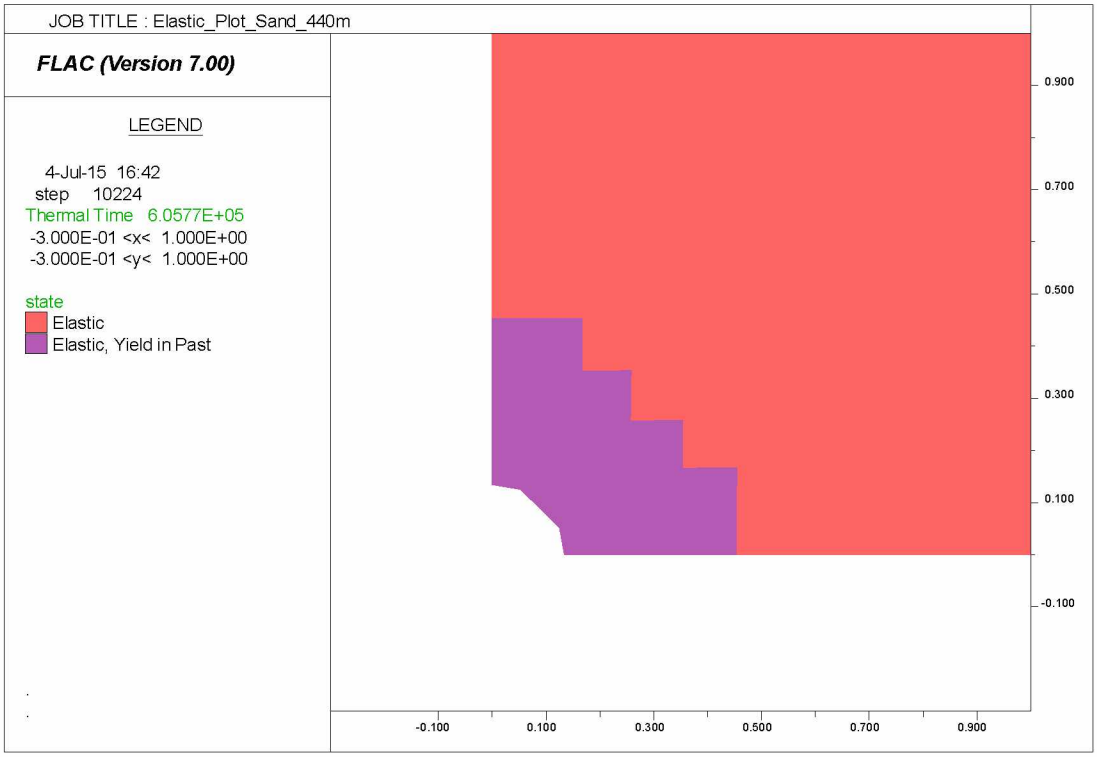

(b)

Figure 23. State of Wellbore in Sand at the Depth of 440m with 2.4 MPa mud pressure on the Wellbore (a) Deformation Plot; (b)State Graph Show Well is Stable

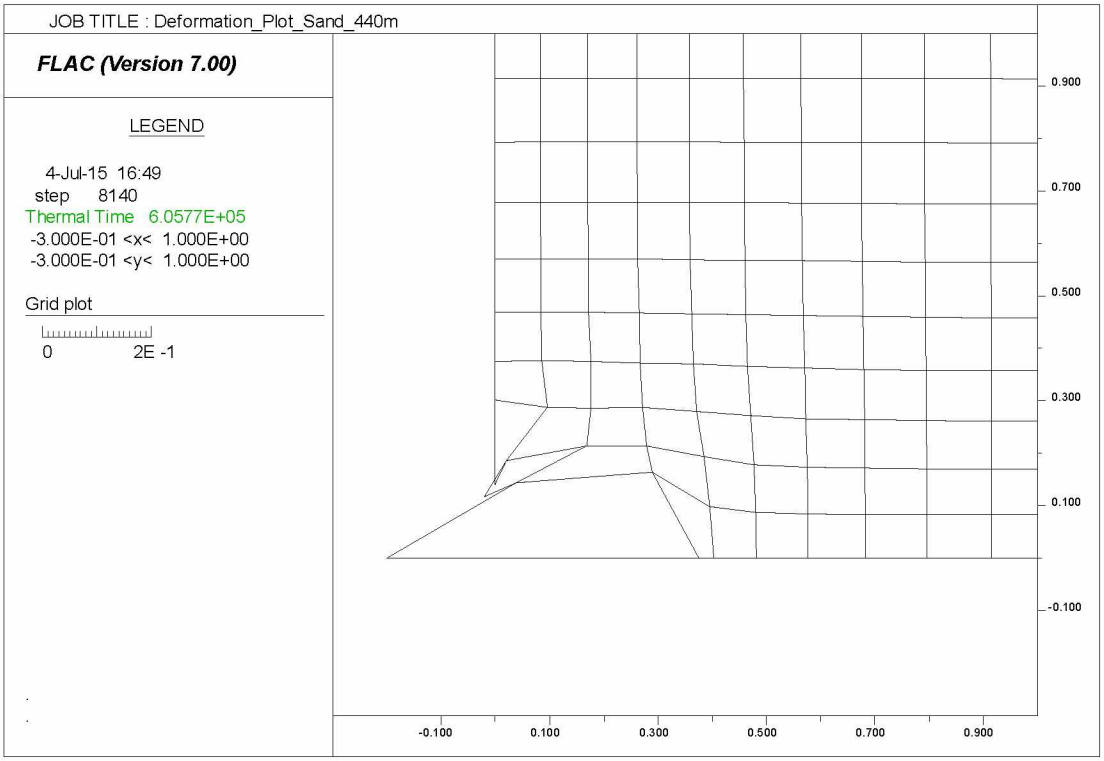

(a)

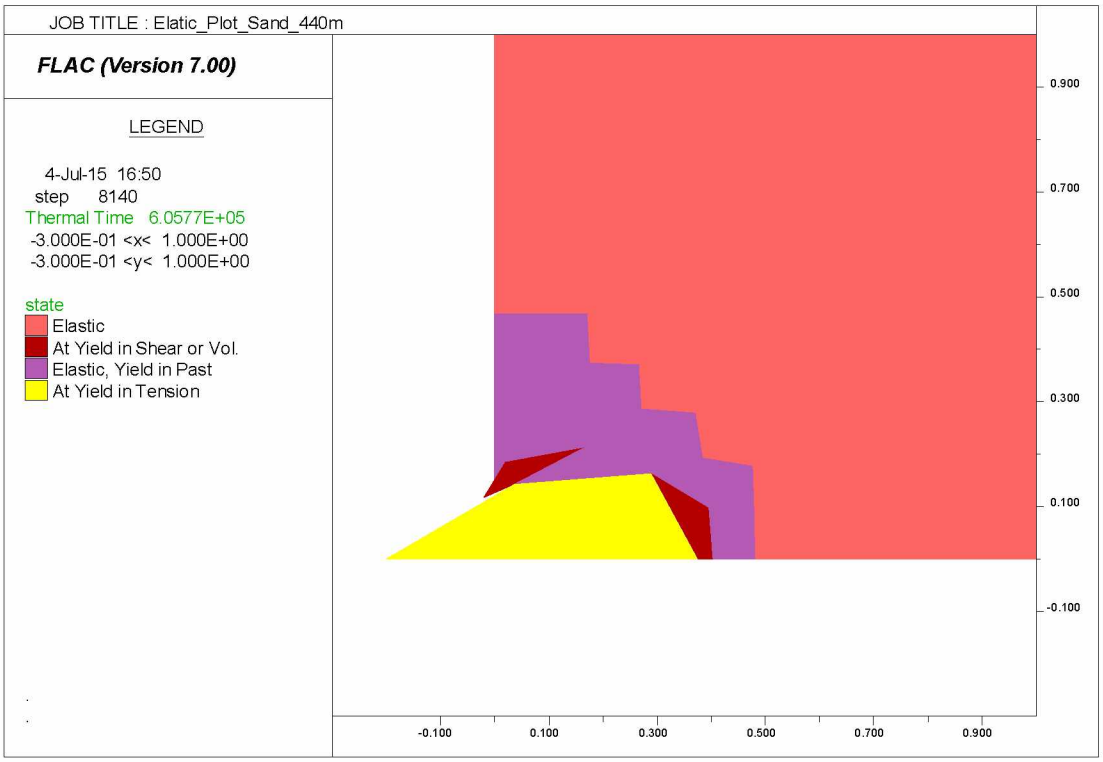

(b)

Figure 24. State of Wellbore in Sand at the Depth of 440m with 2.3 MPa Mud Pressure on the Wellbore (a) Collapsing; (b) State Graph Show Yields

Chapter 5: Simulation Results and Analysis

5.1 Simulation Results

In this study, thicknesses of the three layers in the permafrost formation were selected arbitrarily. It was necessary to check and determine if the layers were under elastic condition at the beginning of the simulation. For example, the silt formation was at a depth from 120 m to 260 m. If the silt formation was lowered to a depth of 280 m, with the same in-situ stress and pore pressure gradient, yield could occur after FLAC run initial equilibrium as elastic model (Figure 25). For real conditions, yield cannot happen before the well was drilled. The state graph should show elastic everywhere. So 260 m would be the maximum depth that silt can reach in this model. After all initial conditions were checked, the three layers simulated in the model were considered reasonable: clay was at a depth from 0 m to 120 m, silt from 120 m to 260 m, and sand from 260 m to 560 m.

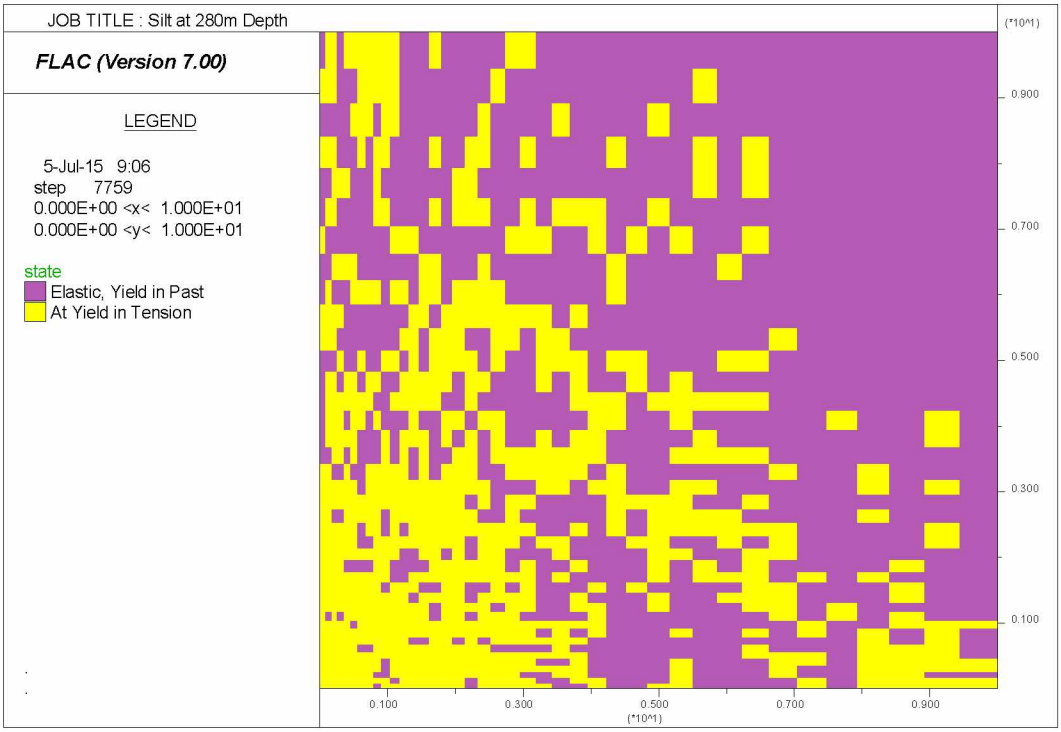

Figure 25. Initial State Graph of Silt at 280m Depth; Yield before drilling

Simulation results minimum wellbore pressure for stability in three different ground formations at different depth and for thermal time of 1 week, 1 month, 1 year, and 5

years are listed in Tables 9 to 12. In some cases, after the minimum wellbore pressure for stability was applied, there was some minor yielding away from the wellbore. For example, the silt formation at the depth of 180 m and thermal time of 1 month stabilized at a minimum wellbore pressure of 2.5MPa, but minor yield could be found approximately 2.5 meters away from the wellbore (Figure 26). This is more than 6 times of the wellbore radius away from the wellbore with minimum or no impact on the wellbore stability. It was, therefore, ignored. The wellbore is considered stable with 2.5MPa mud pressure.

Another situation was that at some tested minimum mud pressure for stability, some small yield points could be found around the wellbore. As these small points do not strongly affect the wellbore stability, tested pressures are still reasonable. Figure 27 is an example of this condition, which shows clay formation at the depth of 120 m and thermal time of 1 week with a stable pressure of 0.6MPa. When casing was added for the well, these minor small yield points were gone.

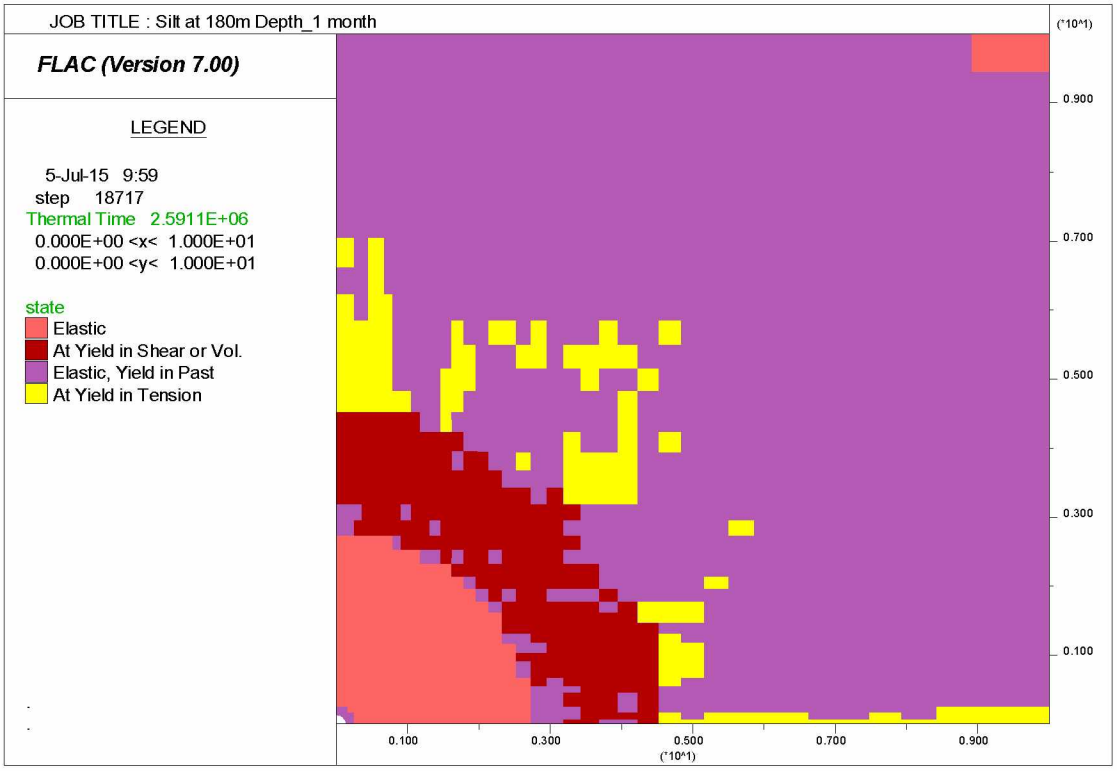

Figure 26. State Graph Shows Yield Far Away from the Wellbore

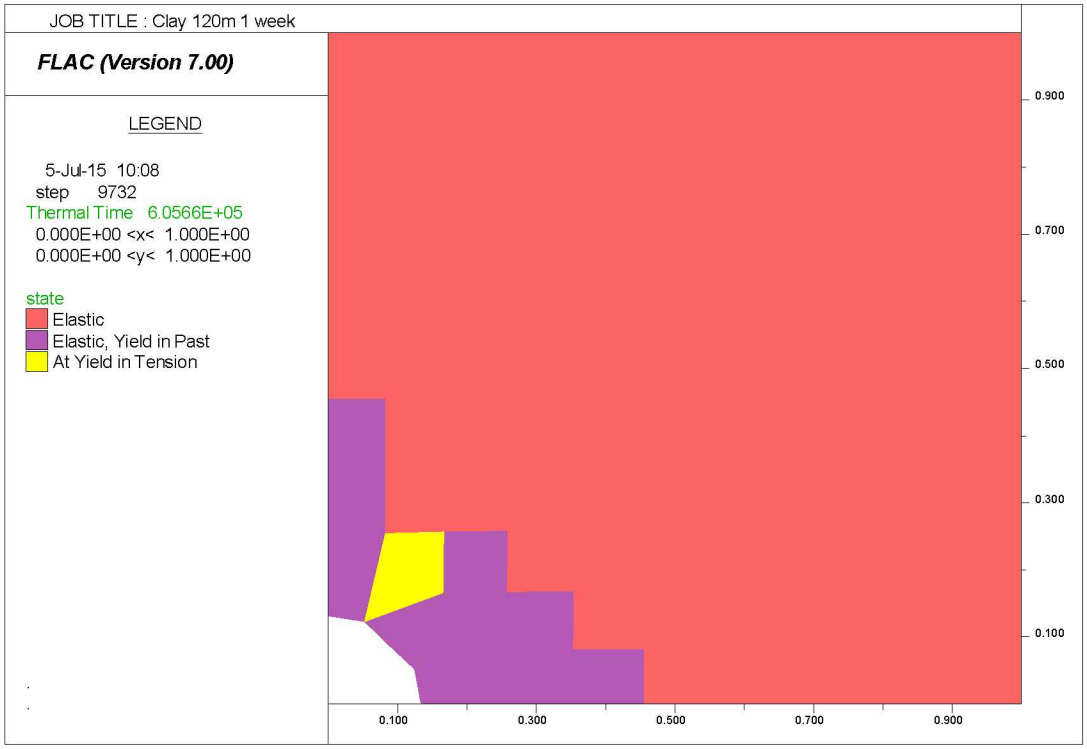

Figure 27. Clay at the Depth of 120m with 0.6 MPa Mud Pressure Applied Shows Small Yield Point around the Wellbore

Table 9: Minimum Stabile Pressure at Thermal Time 1 Week

Layer	Friction Angle	Boundary Temperature	Thaw Radius	Depth	Sxx	Syy	Pore Pressure	Wellbore Pressure
	degree	K	m	m	MPa	MPa	MPa	MPa
Clay	10	267	1.20	20	0.29	0.29	0.20	0.0
	10	267	1.20	40	0.59	0.59	0.41	0.0
	10	267	1.20	60	0.88	0.88	0.61	0.1
	10	267	1.20	80	1.18	1.18	0.82	0.3
	10	267	1.20	100	1.47	1.47	1.02	0.4
	10	267	1.20	120	1.76	1.76	1.22	0.6
Silt	20	267	1.45	120	1.76	1.76	1.22	1.8
	20	267	1.45	140	2.06	2.06	1.43	2.0
	20	267	1.45	160	2.35	2.35	1.63	2.2
	20	267	1.45	180	2.65	2.65	1.84	2.5
	20	267	1.45	200	2.94	2.94	2.04	2.6
	20	267	1.45	220	3.23	3.23	2.24	2.8
	20	267	1.45	240	3.53	3.53	2.45	3.0
	20	267	1.45	260	3.82	3.82	2.65	3.3
Sand	30	267	1.47	260	3.82	3.82	2.65	0.7
	30	267	1.47	280	4.12	4.12	2.86	0.9
	30	267	1.47	300	4.41	4.41	3.06	1.0
	30	267	1.47	320	4.70	4.70	3.26	1.3
	30	267	1.47	340	5.00	5.00	3.47	1.5
	30	267	1.47	360	5.29	5.29	3.67	1.6
	30	267	1.47	380	5.59	5.59	3.88	1.7

	30	267	1.47	400	5.88	5.88	4.08	1.9
	30	267	1.47	420	6.17	6.17	4.28	2.3
	30	267	1.47	440	6.47	6.47	4.49	2.4
	30	267	1.47	460	6.76	6.76	4.69	2.6
	30	267	1.47	480	7.06	7.06	4.90	2.8
	30	267	1.47	500	7.35	7.35	5.10	3.0
	30	267	1.47	520	7.64	7.64	5.30	3.2
	30	267	1.47	540	7.94	7.94	5.51	3.4
	30	267	1.47	560	8.23	8.23	5.71	3.6

Table 10: Minimum Stable Pressure at Thermal Time 1 Month

Layer	**Friction Angle**	**Boundary Temperature**	**Thaw Radius**	**Depth**	**Sxx**	**Syy**	**Pore Pressure**	**Wellbore Pressure**
	degree	**K**	**m**	**m**	**MPa**	**MPa**	**MPa**	**MPa**
Clay	10	267	2.15	20	0.29	0.29	0.20	0.0
	10	267	2.15	40	0.59	0.59	0.41	0.0
	10	267	2.15	60	0.88	0.88	0.61	0.1
	10	267	2.15	80	1.18	1.18	0.82	0.2
	10	267	2.15	100	1.47	1.47	1.02	0.4
	10	267	2.15	120	1.76	1.76	1.22	0.6
Silt	20	267	2.57	120	1.76	1.76	1.22	1.9
	20	267	2.57	140	2.06	2.06	1.43	2.1
	20	267	2.57	160	2.35	2.35	1.63	2.3
	20	267	2.57	180	2.65	2.65	1.84	2.5

	20	267	2.57	200	2.94	2.94	2.04	2.8
	20	267	2.57	220	3.23	3.23	2.24	2.9
	20	267	2.57	240	3.53	3.53	2.45	3.1
	20	267	2.57	260	3.82	3.82	2.65	3.4
Sand	30	267	2.62	260	3.82	3.82	2.65	0.7
	30	267	2.62	280	4.12	4.12	2.86	1.0
	30	267	2.62	300	4.41	4.41	3.06	1.1
	30	267	2.62	320	4.70	4.70	3.26	1.3
	30	267	2.62	340	5.00	5.00	3.47	1.5
	30	267	2.62	360	5.29	5.29	3.67	1.6
	30	267	2.62	380	5.59	5.59	3.88	1.8
	30	267	2.62	400	5.88	5.88	4.08	2.2
	30	267	2.62	420	6.17	6.17	4.28	2.3
	30	267	2.62	440	6.47	6.47	4.49	2.4
	30	267	2.62	460	6.76	6.76	4.69	2.7
	30	267	2.62	480	7.06	7.06	4.90	2.8
	30	267	2.62	500	7.35	7.35	5.10	3.0
	30	267	2.62	520	7.64	7.64	5.30	3.2
	30	267	2.62	540	7.94	7.94	5.51	3.5
	30	267	2.62	560	8.23	8.23	5.71	3.7

Table 11: Minimum Stable Pressure at Thermal Time 1 Year

Layer	Friction Angle	Boundary Temperature	Thaw Radius	Depth	Sxx	Syy	Pore Pressure	Wellbore Pressure
	degree	K	m	m	MPa	MPa	MPa	MPa
Clay	10	268.2	6.60	20	0.29	0.29	0.20	0.0
	10	268.2	6.60	40	0.59	0.59	0.41	0.0
	10	268.2	6.60	60	0.88	0.88	0.61	0.1
	10	268.2	6.60	80	1.18	1.18	0.82	0.2
	10	268.2	6.60	100	1.47	1.47	1.02	0.4
	10	268.2	6.60	120	1.76	1.76	1.22	0.6
Silt	20	269.7	8.00	120	1.76	1.76	1.22	2.4
	20	269.7	8.00	140	2.06	2.06	1.43	2.5
	20	269.7	8.00	160	2.35	2.35	1.63	2.8
	20	269.7	8.00	180	2.65	2.65	1.84	3.0
	20	269.7	8.00	200	2.94	2.94	2.04	3.1
	20	269.7	8.00	220	3.23	3.23	2.24	3.2
	20	269.7	8.00	240	3.53	3.53	2.45	3.4
	20	269.7	8.00	260	3.82	3.82	2.65	3.6
Sand	30	269.6	7.94	260	3.82	3.82	2.65	0.8
	30	269.6	7.94	280	4.12	4.12	2.86	1.1
	30	269.6	7.94	300	4.41	4.41	3.06	1.2
	30	269.6	7.94	320	4.70	4.70	3.26	1.5
	30	269.6	7.94	340	5.00	5.00	3.47	1.7
	30	269.6	7.94	360	5.29	5.29	3.67	1.8
	30	269.6	7.94	380	5.59	5.59	3.88	2.0

	30	269.6	7.94	400	5.88	5.88	4.08	2.3
	30	269.6	7.94	420	6.17	6.17	4.28	2.4
	30	269.6	7.94	440	6.47	6.47	4.49	2.5
	30	269.6	7.94	460	6.76	6.76	4.69	2.8
	30	269.6	7.94	480	7.06	7.06	4.90	2.9
	30	269.6	7.94	500	7.35	7.35	5.10	3.2
	30	269.6	7.94	520	7.64	7.64	5.30	3.3
	30	269.6	7.94	540	7.94	7.94	5.51	3.5
	30	269.6	7.94	560	8.23	8.23	5.71	3.8

Table 12: Minimum Stable Pressure at Thermal Time 5 Years

Layer	**Friction Angle**	**Boundary Temperature**	**Thaw Radius**	**Depth**	**Sxx**	**Syy**	**Pore Pressure**	**Wellbore Pressure**
	degree	**K**	**m**	**m**	**MPa**	**MPa**	**MPa**	**MPa**
Clay	10	273	10.00	20	0.29	0.29	0.20	0.0
	10	273	10.00	40	0.59	0.59	0.41	0.0
	10	273	10.00	60	0.88	0.88	0.61	0.0
	10	273	10.00	80	1.18	1.18	0.82	0.3
	10	273	10.00	100	1.47	1.47	1.02	0.4
	10	273	10.00	120	1.76	1.76	1.22	0.7
Silt	20	273	10.00	120	1.76	1.76	1.22	2.4
	20	273	10.00	140	2.06	2.06	1.43	2.6
	20	273	10.00	160	2.35	2.35	1.63	2.8
	20	273	10.00	180	2.65	2.65	1.84	3.0

	20	273	10.00	200	2.94	2.94	2.04	3.2
	20	273	10.00	220	3.23	3.23	2.24	3.3
	20	273	10.00	240	3.53	3.53	2.45	3.5
	20	273	10.00	260	3.82	3.82	2.65	3.7
Sand	30	273	10.00	260	3.82	3.82	2.65	0.9
	30	273	10.00	280	4.12	4.12	2.86	1.1
	30	273	10.00	300	4.41	4.41	3.06	1.2
	30	273	10.00	320	4.70	4.70	3.26	1.5
	30	273	10.00	340	5.00	5.00	3.47	1.6
	30	273	10.00	360	5.29	5.29	3.67	1.8
	30	273	10.00	380	5.59	5.59	3.88	2.0
	30	273	10.00	400	5.88	5.88	4.08	2.1
	30	273	10.00	420	6.17	6.17	4.28	2.4
	30	273	10.00	440	6.47	6.47	4.49	2.5
	30	273	10.00	460	6.76	6.76	4.69	2.8
	30	273	10.00	480	7.06	7.06	4.90	3.0
	30	273	10.00	500	7.35	7.35	5.10	3.2
	30	273	10.00	520	7.64	7.64	5.30	3.3
	30	273	10.00	540	7.94	7.94	5.51	3.6
	30	273	10.00	560	8.23	8.23	5.71	3.8

From the results, the total tendency of minimum stable pressure at the same depth increases as the thermal time increases for all three materials. Minimum stable pressures in silt formation were much higher than pressures in clay and sand formations. Changing in wellbore radius or the drilling fluid temperature will change the tested mud pressure results. The minimum wellbore mud pressure to maintain stability in permafrost increases as the wellbore radius decreases or fluid temperature increase. Sample FLAC code is presented in Appendix I

From Figure 28, thaw radii before 30 years for sand in this simulation are higher than Smith and Clegg's results showed in Figure 6. The reason for this happened is the initial temperature in the simulation is lower than what Smith and Clegg used. The drilling fluid temperature that Smith and Clegg used is unknown, so drilling fluid temperature difference may another reason for simulated thaw radii higher than reference results. The tendencies of these two lines are same, thermal analysis in this simulation is reasonable.

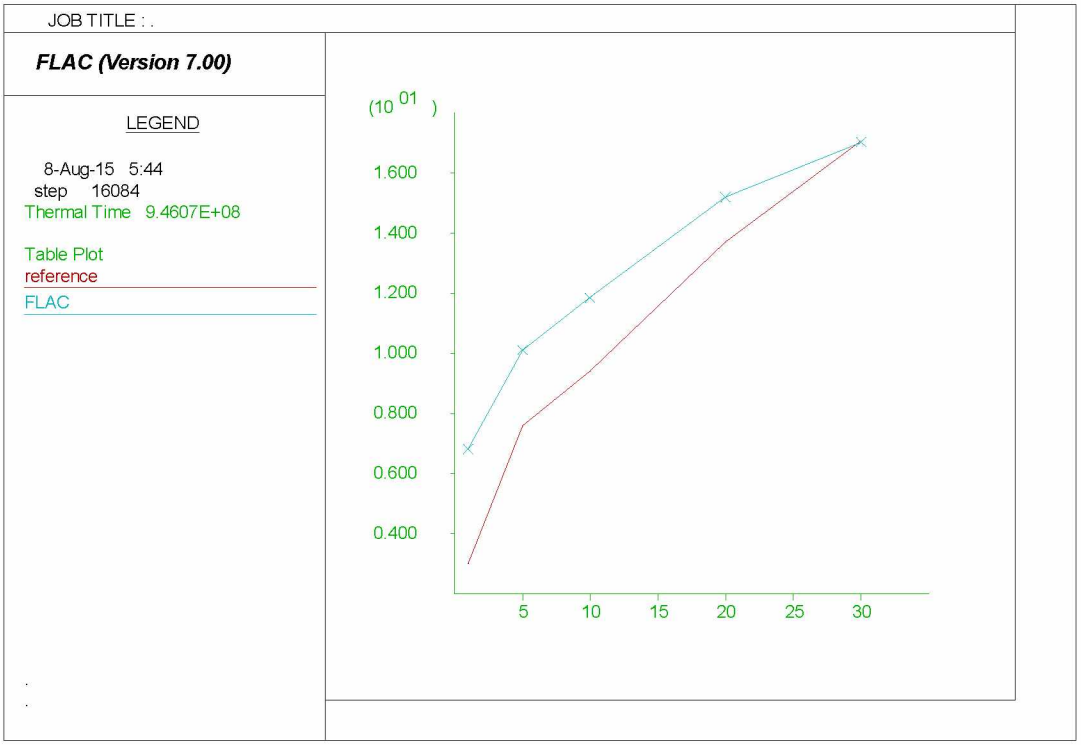

Figure 28. Simulated Thaw Radii Higher than Reference Results

I choose clay at 120 meter depth, silt at 220 meter depth, and sand at 320 meter as three example points to check which property is the most significant to effect the minimum mud pressure for stability. Each property increases 20% individually. Checking thermal time is one week. Test results are shown in Table 13, negative value means decrease and positive value means increase of the minimum mum pressure. For these four properties, pore pressure is the most significant one to influence the minimum mud pressure for stability in frozen soil.

Table 13: Property Change Influence Tested Pressure

Each Property Increase 20%	ΔP (MPa)			Average ΔP (MPa)
	Clay	Silt	Sand	
Pore Pressure	0.3	0.4	0.6	0.43
Initial Cohesion	-0.1	-0.1	-0.5	-0.23
Frictional Angle	-0.1	-0.4	-0.3	-0.27
Fluid Temperature	0.1	0.5	0.1	0.23

5.2 Regression Analysis of Results

After all simulation results were recorded, regression analysis was conducted to find a reasonable function to estimate the minimum wellbore mud pressure to maintain stability in permafrost formation. The statistical analysis reached a R square value of 0.99, indicating a strong relationship between the minimum wellbore mud pressure for stability and the permafrost properties. Statistical indicators of the analysis can be found in Table 13.

Table 14: Regression Analysis Result

Regression Statistics	
Multiple R	0.994619114
R Square	0.989267181
Adjusted R Square	0.988893866
Standard Error	0.122192853
Observations	120

	Coefficients	Standard Error	t Stat	P-value
Intercept	-0.632151276	0.042838219	-14.75671232	2.68E-28
pore P	0.93192471	0.014983982	62.19472836	2.26E-90

cohesion	-1.701195407	0.022981055	-74.02599241	7.4E-99
tan fi	9.05658238	0.218507047	41.44755287	5.55E-71
a	9.17044E-09	1.06062E-09	8.646334951	3.64E-14

Parameter "a" was set based on the result, while the area of the simulation model decreases or drilling fluid temperature increases, the minimum wellbore mud pressure for stability will increases. And to match the unit of tested pressure (MPa), parameter "a" is $\frac{\Delta T(K_{fr}-K_{un})t}{A}$. where ΔT is the temperature difference between fluid and initial temperature in degree Kelvin, K_{fr} and K_{un} are frozen and unfrozen thermal conductivity in W/m/K, respectively, t is thermal time in seconds, and A is the simulation model area. The coefficient of parameter "a" is very low which means at short thermal time, the temperature effect on the wellbore stability can be ignored.

Based on the regression analysis, the minimum wellbore mud pressure for stability can be estimated from the following expression:

$$P_{min} = 0.932P_p - 1.701C + 9.057\tan\varphi + 9.17 \times 10^{-9}\frac{\Delta T(K_{fr} - K_{un})t}{A} - 0.632$$

Where

P_{min} = minimum wellbore stable pressure, MPa

P_p = pore pressure, MPa

C = initial cohesion of permafrost formation, MPa

φ = internal frictional angle, degree

5.3 Stable Pressure after Casing Added

Casing is one of the most important things to keep the wellbore stable during drilling and production. All results from previous simulation did not contain casing around the well, considered to be the case during the drilling phase. This is to investigate the mud pressure requirement for wellbore stability at the drilling stage. When drilling is completed and casing added, it is expected that the stability will be significantly enhanced.

Addition of K55 casing, which is one of the common type and fit the simulated

wellbore radius, was simulated after the minimum wellbore mud pressure was determined. With casing added, all the mud pressures can be reduced to zero and the wellbore would still be stable. In addition as shown in Figure 27, at some simulated mud pressure, small yield point can be found around the wellbore without casing. After casing added, the yield point disappeared (Figure 28). The FLAC code for casing can also be found in Appendix I

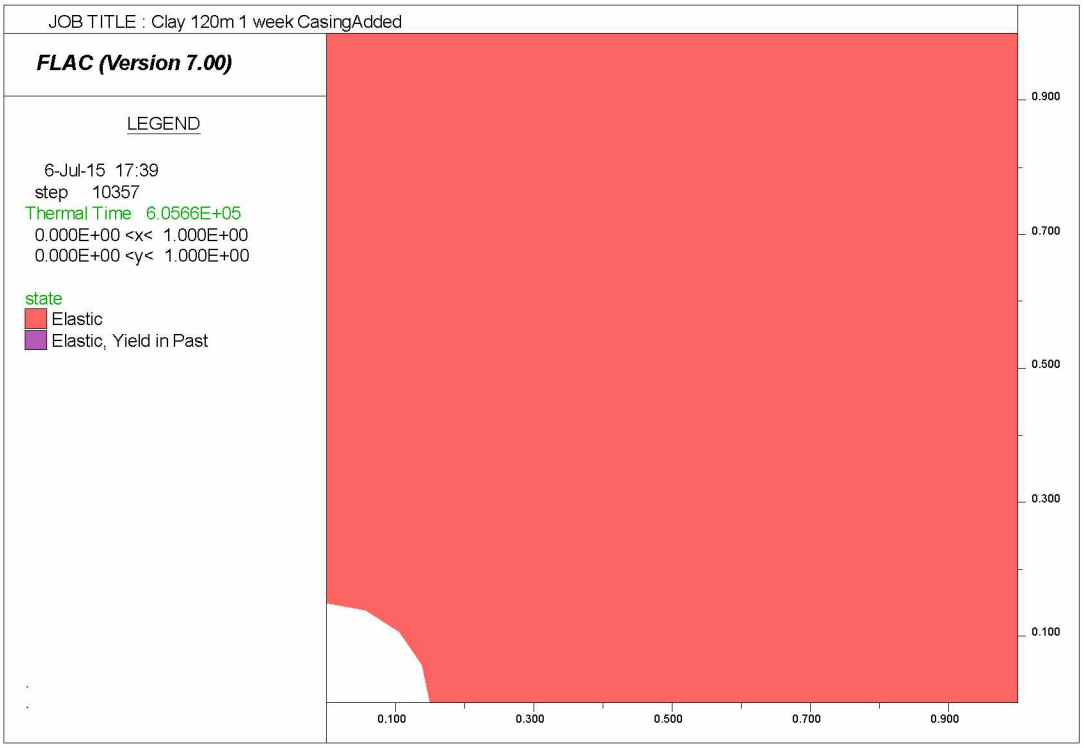

Figure 29. Clay at the depth of 120m with 0.6 MPa Mud Pressure Applied, No Yield Point after Casing Added

Chapter 6: Conclusions and Recommendations

6.1 Conclusions

To better understand the wellbore stability in a permafrost formation, we focused this study on an in situ stress analysis of permafrost. Because of the ice content in permafrost, temperature plays the most significant role in determining permafrost properties. This study investigated the wellbore stability in terms of temperature variations and time. The following conclusions were made based on the simulation results:

1. Three models representing horizontal cut sessions at different depths were built with FLAC for clay, silt, and sand formations respectively. Horizontal stresses applied the simulation were uniform, considering isotropic properties of most permafrost formations.

2. Cohesion was found to be a function of uniaxial compressive strength (UCS) and internal frictional angle as well as temperature variation. The UCS values at different temperatures below freezing were based on Ladanyi's chart (1972, Figure 15).

3. Based on regression analysis of simulation results, the minimum wellbore mud pressure was estimated with a number of variables, including pore pressure (P_p), initial cohesion (C), internal frictional angle (φ), temperature difference between formation and fluid (ΔT), conductivity difference frozen and unfrozen ground materials ($K_{fr} - K_{un}$), thermal time (t), and model area (A). Pore pressure has the strongest effect for the pressure value and in a short operation time, effect of high temperature drilling fluid can be ignored.

4. The K55 casing was also simulated for wellbore stability in permafrost. With casing added, the mud pressure may drop to 0MPa and the wellbore will still maintain stability. The addition of casing significantly improved the ground

condition as compared with that without casing.

6.2 Recommendations

Errors were inevitable in this simulation because of data limitation. The properties for the simulated permafrost formation were obtained from different references and with different assumptions. Other values such as UCS and conductivity were read from figures that may not be exact.

Water content is very important in permafrost. However, the simulation software FLAC is not capable of modeling the water content in the ground formation directly. The approximation in modeling permafrost with various water contents is by assigning thermal conductivities as a function of water content. Similarly, the latent heat of the formation cannot be directly simulated either. Approximation was made in the model by assigning a high specific heat value at ice melting point between 272K to 274K to account for the latent heat of permafrost. All these assumptions were reasonable approximations, but may induce some errors.

For all the simulations conducted in this study, one quarter section of the wellbore was used with the assumption that the wellbore model was axial symmetry. This significantly reduced the effort in conducting the simulation work.

Despit of the possible errors, the estimated minimum wellbore mud pressure for stability in permafrost formation is believed reasonable. For further study, simulations with real well data to check the statistical model may be necessary. A better approach for handling water content and latent heat in the model may also improve the accuracy of the simulation results.

Appendix

Appendix I: FLAC Code Explanation

density = formation density, kg/m^3

bulk = bulk modulus (calculate from Young's modulus and Poisson's ratio automatically), Pa

shear = shear modulus (calculate from Young's modulus and Poisson's ratio automatically), Pa

cohesion = initial cohesion at formation temperature, Pa

friction = internal frictional angle, degree

dilation = dilation angle, degree

tension = tension stress, Pa

sxx and syy = horizontal stresses, Pa

pp = pore pressure, Pa

spec_heat = specific heat, J/kg/K

thexp = coefficient of linear thermal expansion

temp (i,j) = temperature at grid point (i,j)

Appendix II: FLAC Code Examples for Simulation

1. Clay at 120m depth, thermal time 1 week

"Step 1: Initial Mechanical Equilibrium"

config thermal

grid 40,40

model elastic

gen 0.0,0.0 0.0,10.0 10.0,10.0 10.0,0.0 i=1,41 j=1,41 rat 1.05 1.05

gen arc 0.0,0.0 0.15,0.0 90.0

group 'Clay:Clay' notnull

model mohr notnull group 'Clay:Clay'

prop density=1900.0 bulk=1.56667E9 shear=7.23077E8 cohesion=849000.0 friction=10 dilation=10.0 tension=253000.0 notnull group 'Clay:Clay'

```
apply sxx -1760000.0 from 41,41 to 41,1
apply syy -1760000.0 from 1,41 to 41,41
initial pp 1220000.0
fix    x i 1
fix    y j 1
set thermal=off mech on
history 999 unbalanced
solve    elastic

"Step 2: Thermal Analysis"
set thermal=on mech=off
model th_isotropic
prop conductivity= 2.35 spec_heat=1100 thexp=69E-6
initial temperature 267
model null i 1 j 1 2
group 'null' i 1 j 1 2
group delete 'null'
model null i 2 j 1
group 'null' i 2 j 1
group delete 'null'
fix    temperature 267 j 41
fix    temperature 267 i 41
fix    temperature 343.0 mark
table 2 267,1100 270,1100 272,1100 273,3e4 274,3e4 275,1460 275,1460 343,1460
def mon_spec_heat
   whilestepping
   loop i (1,izones)
   loop j (1,jzones)
   if model(i,j) # 1
      _temp = (temp(i,j)+temp(i+1,j)+temp(i,j+1)+temp(i+1,j+1))/4.
```

```
      spec_heat(i,j)=table(2,_temp)
   endif
   endloop
   endloop
end
mon_spec_heat
table 10086 243,2.35 263,2.35 272,2.35 273,1.50 274,1.50 294,1.50 400,1.50
def adjust_conductivity
   loop i (1, izones)
   loop j (1, jzones)
   if model(i,j) # 1
      _temp = (temp(i,j)+temp(i+1,j)+temp(i,j+1)+temp(i+1,j+1))/4.
      conductivity(i,j)=table(10086,_temp)
   endif
   endloop
   endloop
end
adjust_conductivity
solve age 6.05e5

"Step 3: Minimum Wellbore Stable Pressure Test"
set mechanical=on thermal=off
set=large
table 10087 253.15,1.55e6 258.15,1.25e6 263.15,1.01e6 269.15,0.78e6 271.15,0.73e6
273.15,0.68e6 343,0.68e6
def adjust_cohesion
   loop i (1,izones)
   loop j (1,jzones)
   if model(i,j) # 1
      _temp = (temp(i,j)+temp(i+1,j)+temp(i,j+1)+temp(i+1,j+1))/4.
```

```
        cohesion(i,j)= table(10087,_temp)
    endif
    endloop
    endloop
end
adjust_cohesion
table 10088    263,1.88e9 272,1.88e9 273,1.88e9 274,1.88e7 293,1.88e7
def adjust_KG
    _prat = 0.3
    loop i (1,izones)
    loop j (1,jzones)
    if model(i,j) # 1
        _temp = (temp(i,j)+temp(i+1,j)+temp(i,j+1)+temp(i+1,j+1))/4.
        _ymod = table(10088,_temp)
        shear_mod(i,j) = _ymod/(2.*(1. + _prat))
        bulk_mod(i,j) = 3.*_ymod/(1.-2.*_prat)
    endif
    endloop
    endloop
end
adjust_KG
apply pressure 600000.0 from 1,3 to 3,1
solve
```

2. Silt at 180m, thermal time 1 month

```
"Step 1: Initial Mechanical Equilibrium"
config thermal
grid 40,40
model elastic
```

```
gen 0.0,0.0 0.0,10.0 10.0,10.0 10.0,0.0 i=1,41 j=1,41 rat 1.05 1.05
gen arc 0.0,0.0 0.15,0.0 90.0
group 'Silt:Silt' notnull
model mohr notnull group 'Silt:Silt'
prop density=2000.0 bulk=7.33333E9 shear=3.38462E9 cohesion=1030000.0
friction=20.0 dilation=10.0 tension=368000.0 notnull group 'Silt:Silt'
apply sxx -2650000.0 from 41,41 to 41,1
apply syy -2650000.0 from 1,41 to 41,41
initial pp 1840000.0
fix x i 1
fix y j 1
set thermal=off mech on
history 999 unbalanced
solve elastic

"Step 2: Thermal Analysis"
set thermal=on mech=off
model th_isotropic
prop conductivity= 2.67 spec_heat=1050 thexp=69E-6
initial temperature 267
model null i 1 j 1 2
group 'null' i 1 j 1 2
group delete 'null'
model null i 2 j 1
group 'null' i 2 j 1
group delete 'null'
fix temperature 267 j 41
fix temperature 267 i 41
fix temperature 343.0 mark
table 2 267,1050 270,1050 272,1050 273,3e4 274,3e4 275,3e4 275,1430 343,1430
```

```
def mon_spec_heat
   whilestepping
   loop i (1,izones)
   loop j (1,jzones)
   if model(i,j) # 1
      _temp = (temp(i,j)+temp(i+1,j)+temp(i,j+1)+temp(i+1,j+1))/4.
      spec_heat(i,j)=table(2,_temp)
   endif
   endloop
   endloop
end
mon_spec_heat
table 10086 243,2.67 263,2.67 272,2.67 273,1.64 274,1.64 294,1.64 400,1.64
def adjust_conductivity
   loop i (1, izones)
   loop j (1, jzones)
   if model(i,j) # 1
      _temp = (temp(i,j)+temp(i+1,j)+temp(i,j+1)+temp(i+1,j+1))/4.
      conductivity(i,j)=table(10086,_temp)
   endif
   endloop
   endloop
end
adjust_conductivity
solve age 2.59e6

"Step 3: Minimum Wellbore Stable Pressure Test"
set mechanical=on thermal=off
set=large
table 10087 253.15,3.43e6 258.15,2.57e6 263.15,1.72e6 269.15,0.69e6 271.15,0.34e6
```

```
273.15,0.26e6 343,0.26e6
def adjust_cohesion
   loop i (1,izones)
   loop j (1,jzones)
   if model(i,j) # 1
      _temp = (temp(i,j)+temp(i+1,j)+temp(i,j+1)+temp(i+1,j+1))/4.
      cohesion(i,j)= table(10087,_temp)
   endif
   endloop
   endloop
end
adjust_cohesion
table 10088    263,8.8e9 272,8.8e9 273,8.8e9 274,8.8e7 293,8.8e7
def adjust_KG
   _prat = 0.3
   loop i (1,izones)
   loop j (1,jzones)
   if model(i,j) # 1
      _temp = (temp(i,j)+temp(i+1,j)+temp(i,j+1)+temp(i+1,j+1))/4.
      _ymod = table(10088,_temp)
      shear_mod(i,j) = _ymod/(2.*(1. + _prat))
      bulk_mod(i,j) = 3.*_ymod/(1.-2.*_prat)
   endif
   endloop
   endloop
end
adjust_KG
apply pressure 2500000.0 from 1,3 to 3,1
solve
```

3. Sand 440m, thermal time 1 year

"Step 1: Initial Mechanical Equilibrium"

```
config thermal
grid 40,40
model elastic
gen 0.0,0.0 0.0,10.0 10.0,10.0 10.0,0.0 i=1,41 j=1,41 rat 1.05 1.05
gen arc 0.0,0.0 0.15,0.0 90.0
group 'User:Ottawa Sand' notnull
model mohr notnull group 'User:Ottawa Sand'
prop density=2100.0 bulk=1.08333E10 shear=5E9 cohesion=3750000.0 friction=30
dilation=10.0 tension=1620000.0 notnull group 'User:Ottawa Sand'
apply sxx -6470000.0 from 41,41 to 41,1
apply syy -6470000.0 from 1,41 to 41,41
initial pp 4490000.0
fix   x i 1
fix   y j 1
set thermal=off mech on
history 999 unbalanced
solve   elastic
```

"Step 2: Thermal Analysis"

```
set thermal=on mech=off
model th_isotropic
prop conductivity= 3.59 spec_heat=1070 thexp=69E-6
initial temperature 267
model null i 1 j 1 2
group 'null' i 1 j 1 2
group delete 'null'
```

```
model null i 2 j 1
group 'null' i 2 j 1
group delete 'null'
fix    temperature 271 j 41
fix    temperature 271 i 41
fix    temperature 343.0 mark
table 2 267,1070 270,1070 272,1070 273,3e4 274,3e4 275,3e4 275,1470 343,1470
def mon_spec_heat
   whilestepping
   loop i (1,izones)
   loop j (1,jzones)
   if model(i,j) # 1
      _temp = (temp(i,j)+temp(i+1,j)+temp(i,j+1)+temp(i+1,j+1))/4.
      spec_heat(i,j)=table(2,_temp)
   endif
   endloop
   endloop
end
mon_spec_heat
table 10086 243,3.59 263,3.59 272,3.59 273,2.17 274,2.17 294,2.17 400,2.17
def adjust_conductivity
   loop i (1, izones)
   loop j (1, jzones)
   if model(i,j) # 1
      _temp = (temp(i,j)+temp(i+1,j)+temp(i,j+1)+temp(i+1,j+1))/4.
      conductivity(i,j)=table(10086,_temp)
   endif
   endloop
   endloop
end
```

```
adjust_conductivity
solve age 3.15e7

"Step 3: Minimum Wellbore Stable Pressure Test"
set mechanical=on thermal=off
set=large
table 10087 253.15,7.67e6 258.15,6.54e6 263.15,5.12e6 269.15,2.98e6 271.15,2.15e6
273.15,1.26e6 343,1.26e6
def adjust_cohesion
   loop i (1,izones)
   loop j (1,jzones)
   if model(i,j) # 1
      _temp = (temp(i,j)+temp(i+1,j)+temp(i,j+1)+temp(i+1,j+1))/4.
      cohesion(i,j)= table(10087,_temp)
   endif
   endloop
   endloop
end
adjust_cohesion
table 10088    263,13.2e9 272,13.2e9 273,13.2e9 274,13.2e7 293,13.2e7
def adjust_KG
   _prat = 0.3
   loop i (1,izones)
   loop j (1,jzones)
   if model(i,j) # 1
      _temp = (temp(i,j)+temp(i+1,j)+temp(i,j+1)+temp(i+1,j+1))/4.
      _ymod = table(10088,_temp)
      shear_mod(i,j) = _ymod/(2.*(1. + _prat))
      bulk_mod(i,j) = 3.*_ymod/(1.-2.*_prat)
   endif
```

```
   endloop
   endloop
end
adjust_KG
apply pressure 2500000.0 from 1,3 to 3,1
solve
```

4. Casing code, add after "adjust_KG" in previous example

```
struct node 1 grid 1,3
struct node 2 grid 2,3
struct node 3 grid 2,2
struct node 4 grid 3,2
struct node 5 grid 3,1
struct liner begin node 1 end node 2 seg 1 prop 5001
struct liner begin node 2 end node 3 seg 1 prop 5001
struct liner begin node 3 end node 4 seg 1 prop 5001
struct liner begin node 4 end node 5 seg 1 prop 5001
struct prop 5001 e=2.1e11 pratio=0.27 area=0.13 thickness=0.01 i=0.0013 shape=0.5
density=6525 thexp=1.2e-7
solve
```

References

1. Andersland, Orlando B., and Branko, Ladanyi, 2004, "Frozen Ground Engineering" Second Edition, John Wiley & Sons, Inc., Hoboken, New Jersey.
2. Benge, O. G., et.al., 1982, "A new Low-Cost Permafrost Cementing System", SPE-10757.
3. Borivoje, Nediljka, and Davorin, 2007, *"Wellbore Instability: Causes and Consequences"*, University of Zagreb, Faculty of Mining, Geology and Petroleum Engineering.
4. Brady, B. H. G, and E. T., Brown, 2006, "Rock Mechanics for Underground Mining." third edition, Dordrecht, The Netherlands: Springer
5. Cheatham Jr., J.B., 1984, *"Wellbore Stability"*, Society of Petroleum Engineering, SPE-13340-PA, **http://dx.doi.org/10.2118/13340-PA**
6. Deily, F. H., and T. C., Owens, 1969, "Stress Around a Wellbore", Society of Petroleum Engineers, SPE-2557-MS, **http://dx.doi.org/10.2118/2557-MS**.
7. Farouki, Omar T., 1981, "Thermal Properties of Soil", United States Army Corps of Engineers, Cold Regions Research and Engineering Laboratory, Hanover, New Hampshire, U.S.A.
8. Ferrians, Oscar J., Jr., 1994, "*Permafrost in Alaska*", The Geology of Alaska: Boulder, Colorado, Geological Society of America, The Geology of North America, Volume. G-1.
9. FLAC, version 7.0. "Theory and Background." Itasca Consulting Group
10. Goodman, Malcolm A., 1978, "World Oil's Handbook of Artic Well Completions", World Oil.
11. Immerstein Tonje, 2013, "Wellbore Stability and Rock Mechanics Study on the Ula field", Master's Thesis, University of Stavanger.
12. Jin, Yan, and Chen, Mian, 2012. "Mechanics of Wellbore Stability." China: Science Press
13. Jorgenson, M. T., T. E., Osterkamp, 2009, *"Permafrost Conditions and Processes"*, Geological Monitoring: Boulder, Colorado, Geological Society of America, page 205-227.

14. Kanevskiy, Z. Mikhail, et.al., 2011, "*Permafrost of Northern Alaska*", International Society of Offshore and Polar Engineers, ISOPE-I-11-077.
15. Luo, Dan, 2014, "Simulation and Analysis of Wellbore Stability Using FLAC for Horizontal Well Drilling in Shale Formations", American Rock Mechanics Association, ARMA-2014-7203
16. Ladanyi, Branko, 1972, "An Engineering Theory of Creep of Frozen Soils", Canadian Geotechnical Journal, Volume 9, Page 63.
17. McLellan, P. J., "Feasibility of Determining In-situ Stresses in Permafrost of the Mackenzie Delta, Northwest Territories", Advanced Geotechnology Inc., Calgary.
18. Osterkamp, T. E., 2003, *"A Thermal History of Permafrost in Alaska"*, Swets& Zeitlinger Lisse.
19. Perkins T.K., et.al., 1975, "Solutions for Some Problems Resulting from Refreezing of permafrost around a Wellbore", American Petroleum Institute, API-75-A001
20. Rutqvist, J., et.al., 2009, "Geomechanical response of permafrost-associated hydrate deposits to depressurization-induced gas production", https://escholarship.org/uc/item/5dh9t42d
21. Shur, Y. L., and C. L. Ping, 1994, "Permafrost dynamics and soil formation, in Proceedings of the Meetings on the Classification, Correlation, and Management of Permafrost-Affected Soils", edited by J. M. Kimble, andR. J. Ahrens, pp. 112–117, USDA Soil Conserv. Serv.-Nat. Soil Surv. Cent.,Lincoln, Neb.
22. Shur, Yuri, 2014, "Introduction of Permafrost Engineering Courseware", University of Alaska Fairbanks.
23. Smith, Robert E., and Clegg, Michael W., 1971, "Analysis and Design of Production Wells Through Thick Permafrost", World Petroleum Congress, WPC-14244.
24. Tsytovich, N. A., "The Mechanics of Frozen Ground" Hardcover edition, Chapter IV and Chapter V, McGraw-Hill Inc.,US.

25. TWISS, R. J., and MOORES, E. M., 2006, "Structural Geology", New York, W. H. Freeman and Company. ULA TAMBAR SUBSURFACE TEAM 2013. Ula Hub Development. BP.

26. Wikipedia, 2015, Young's Modulus (Jun. 25th, 2015 version), https://en.wikipedia.org/wiki/Young%27s_modulus

27. Yang, Zhaohui Joey, et.al., 2010, "Effects of Permafrost and Seasonally Frozen Ground on the Seismic Response of Transportation Infrastructure Sites", Report for Alaska University Transportation Center, INE/AUTC 11.03, Alaska Department of Transportation, FHWA-AK-RD-10-02